A crucial role for dynamic expression of components encoding the negative arm of the circadian clock

Bin Wang [1] ✉, Xiaoying Zhou[1], Arminja N. Kettenbach [2], Hugh D. Mitchell[3,4], Lye Meng Markillie [3,4], Jennifer J. Loros[1,2] & Jay C. Dunlap [1] ✉

In the *Neurospora* circadian system, the White Collar Complex (WCC) drives expression of the principal circadian negative arm component *frequency* (*frq*). FRQ interacts with FRH (FRQ-interacting RNA helicase) and CKI, forming a stable complex that represses its own expression by inhibiting WCC. In this study, a genetic screen identified a gene, designated as *brd-8*, that encodes a conserved auxiliary subunit of the NuA4 histone acetylation complex. Loss of *brd-8* reduces H4 acetylation and RNA polymerase (Pol) II occupancy at *frq* and other known circadian genes, and leads to a long circadian period, delayed phase, and defective overt circadian output at some temperatures. In addition to strongly associating with the NuA4 histone acetyltransferase complex, BRD-8 is also found complexed with the transcription elongation regulator BYE-1. Expression of *brd-8, bye-1, histone h2a.z*, and several NuA4 subunits is controlled by the circadian clock, indicating that the molecular clock both regulates the basic chromatin status and is regulated by changes in chromatin. Taken together, our data identify auxiliary elements of the fungal NuA4 complex having homology to mammalian components, which along with conventional NuA4 subunits, are required for timely and dynamic *frq* expression and thereby a normal and persistent circadian rhythm.

Circadian clocks control a wide variety of physiological, biochemical, and behavioral processes in most eukaryotes and certain prokaryotes. At the molecular level, circadian systems are composed of positive and negative arms and the latter repress their own expression through inhibiting the positive arm. In *Neurospora*, the White Collar Complex (WCC) formed by WC-1 and WC-2 transcriptionally activates the pacemaker gene, *frequency* (*frq*), by binding to two promoter elements: *Clock box* (*C-box*) in the dark and *Proximal Light-Response Element* (*pLRE*) in the light[1–3]. FRQ, the *frq* gene product, associates with FRH (FRQ-interacting RNA helicase)[4,5] and CKI (casein kinase I)[6,7] to form the FFC complex, promoting WCC phosphorylation at a group of residues[6,8,9] to repress its activity and thereby close the feedback loop.

frq is strongly activated in the light and is rhythmically transcribed and translated in the dark[10], events that are highly regulated and whose progress impacts timekeeping; *frq* lies in a region of highly accessible chromatin associated with rapid nucleosome turnover when active[11]. In chromatin, nucleosomes impede transcription initiation by Pol II by inhibiting assembly of the preinitiation complex (PIC) at the promoter[12]. The positive charges on lysine residues of histones can be neutralized by acetylation, which weakens histone-DNA interactions and reduces accessibility to other proteins relevant to gene expression[13]. Acetylation also provides recognition sites for chromatin remodeling complexes bearing bromodomains[14]. Nucleosomes can inhibit transcription elongation by Pol II, and their displacement at

coding sequences directly correlates with the transcription pace of Pol II[15]. The major histone acetyltransferase for histones H4, H2A, and H2A.Z[16–19] in yeast is the thirteen subunit 1.3 MDa NuA4 (Nucleosome acetyltransferase of histone H4) complex, and its catalytic subunit is Esa1. NuA4 is recruited both to gene promoters and coding regions and stimulates the passage of elongating Pol II in transcription initiation and elongation by loosening DNA-histone contacts[20]. Evidence suggests that most histone acetylation at promoter regions precedes and is independent of transcription. In humans, the orthologous Tip60 complex that bears HAT activity is a multiprotein complex with at least 16 subunits[21,22], and may have arisen as a fusion form of two yeast HAT complexes NuA4 and SWR, the multi-subunit complex that incorporates histone variant H2A.Z into chromatin[21]. In addition to histones, TIP60 acetylates BMAL1 in the mammalian clock, providing a docking site that brings the BRD4-P-TEFb complex to DNA-bound BMAL1, promoting release of Pol II and elongation of circadian transcripts[23]. The BYpass of Ess1 (BYE1) protein is a *Saccharomyces cerevisiae* transcription elongation factor[24,25] whose human homologs are PHF3 and DIDO[26]. BYE-1 interacts with Pol II and can positively or negatively regulate transcription elongation[24–26]. Histone H4 acetylation determines chromatin higher-order structure and functional interactions between remodeling enzymes and the chromatin fibers[27]; disruption of Tip60 or NuA4 and impairment of histone H4 acetylation have been implicated in DNA damage repair, plant developmental processes, behavioral variability, neurodegenerative diseases, cell cycle progression, cancer, and ageing[28–44].

In this study, we have identified a conserved bromodomain-containing NuA4-associated subunit, BRD-8, which is required for the NuA4 HAT activity on histone H4 at multiple loci including *frq* and is required for normal *frq* expression, period determination, and persistence of rhythmicity. BRD-8 also complexes with an ortholog of Saccharomyces BYE-1, suggesting a connection to transcription elongation. In the absence of *brd-8*, both histone acetylation and Pol II levels at *frq* are sharply reduced, consistent with reduced expression of *frq*. Interestingly, expression of *brd-8*, *bye-1*, and several NuA4 subunits is controlled by the circadian clock, forming a nested feedback loop surrounding the core transcription translation feedback loop. These and prior data are consistent with an important role for robust and timely transcription of the negative arm proteins in the circadian feedback loop and suggest a link between the circadian clock and the basic transcriptional machinery.

Results

Loss of *brd-8* impacts the *Neurospora* clock
To identify genes regulating the circadian clock, single gene deletion strains of *Neurospora*[45] were screened on race-tube medium bearing menadione which facilitates visualization of the circadian phenotypes[46]. Two deletion strains lacking the same gene, *ncu09482* (now designated as *brd-8*, see below), displayed an arrhythmic overt conidiation phenotype on race tubes (Fig. 1a). To verify the circadian phenotype observed using menadione, Δ*brd-8* was backcrossed to the *ras-1*[bd] and *frq C-box*-driven *luciferase* reporters that have been widely used to visualize overt rhythms and continuously report changes in WCC activity within the core clock respectively. Δ*brd-8* in the *ras-1*[bd] background showed a ~ 3 h longer period with a slightly reduced growth rate for the first three days and subsequently became arrhythmic by both race tube and luciferase assays (Fig. 1a and Supplementary Fig. 1). Consistent with this, the robustness of the *frq C-box*-driven *luciferase* reporter was also dramatically impaired after three days in Δ*brd-8* (Fig. 1a and Supplementary Fig. 2). The long period phenotype was not rescued when medium having a lower concentration (0.01%) of glucose (Supplementary Figures 1 and 2) was used to reduce conidiation and thereby better visualize the overt rhythm; a ~ 3-h phase delay was also observed in Δ*brd-8* (Fig. 1a), and the reduced *frq C-box*-driven bioluminescence signal is consistent with reduced *C-box*-

driven expression which would lead to reduced *frq* expression. Circadian clocks maintain their period lengths across a range of physiological temperatures. To test the performance of Δ*brd-8* at different temperatures, circadian periods of WT and Δ*brd-8* were examined at 20°, 25°, and 30 °C (Fig. 1b); Δ*brd-8* displays arrhythmic overt phenotypes at 30 °C in media bearing either a high (0.1%) or low (0.01%) percentage of glucose (Supplementary Fig. 1), whereas it is rhythmic at all temperatures tested by luciferase analyses (Supplementary Fig. 2), suggesting that *brd-8* also controls the circadian output at high temperature independent of its role in regulating the period length.

In addition to its role as the major transcription factor for *frq*, WC-1 is also the principal blue-light photoreceptor for the organism, directly or indirectly mediating light-induced gene expression[47]. Interestingly, the Δ*brd-8* strain that displayed a ~25-h period and delayed dark FRQ expression retains its capacity to detect light to induce expression of light-responsive genes (Supplementary Figure 3). Unexpectedly, light-induced expression of some genes (e.g. *frq*, *vvd*, *csp-1*, and *sub-1*) is even significantly higher in Δ*brd-8* than in WT, consistent with differing roles for BRD-8 depending on the promoter element (*C-box* vs. *pLRE*) used.

FRQ and WC-1 levels are reduced in the mutant in the dark
To understand the role of BRD-8 at a mechanistic level, core circadian component expression was examined by Western blotting (Fig. 1c). FRH and WC-2 levels are normal or slightly reduced in Δ*brd-8*, and consistent with the long period of Δ*brd-8*, new FRQ in Δ*brd-8* appears later than that in WT and is slightly reduced. However, the level of WC-1 in Δ*brd-8* is significantly reduced. Active WC-1 is unstable and FRQ, by inactivating WCC, stabilizes WC-1[5,6], so to test whether the low WC-1 level is caused by a defective negative arm, Δ*brd-8* was backcrossed to the loss of function allele *frq*[9]; WC-1 levels are further reduced in the *frq*[9]; Δ*brd-8* double mutant (Fig. 1d), which indicates that *brd-8* regulates WC-1 expression at least partially independently of the negative feedback loop. Reduced WC-1 levels as seen in Δ*brd-8* can result in modestly long circadian periods[48]. To test whether the long circadian period in Δ*brd-8* is caused by the reduced WC-1 level, the native promoter of *wc-1* in Δ*brd-8* was replaced by the strongly inducible *qa-2* promoter. In the presence of inducer (quinic acid, QA), the *wc-1* and WC-1 levels are raised to those in WT (Fig. 1e, f) or even higher, but the period defect of Δ*brd-8* is not rescued (Fig. 1g), indicating that the longer period in the mutant is not caused by the low WC-1 level. Similarly, to test whether changes in FRQ levels underlie the long period of Δ*brd-8*, a second copy of the *frq* gene with its native promoter was inserted at the *csr* locus of Δ*brd-8*. The long period of Δ*brd-8* was rescued to WT (Fig. 1h), indicating that reduced *frq* expression in Δ*brd-8* is the cause of the long period length.

BRD-8 is a nonessential subunit of the histone acetyltransferase NuA4 complex and interacts with elongation factor BYE-1
To understand how loss of *brd-8* impacts the circadian clock, BRD-8 was C-terminally epitope-tagged with V5, 10 x histidine, and 3 x FLAG (VHF tag) and purified from protein extracts; three distinct protein bands from the stained gel removed and analyzed by tandem mass spectrometry proved to be proteins encoded by NCU09482 (BRD-8, see below), NCU06787 (ortholog of the NuA4 subunit EAF-3), and NCU05943 (ortholog of the regulator of transcription elongation BYE-1[24]), (left gel, Fig. 2a). To recover more interactors and particularly those with enzymatic activities, NCU09482 (BRD-8) tagged with V5 was isolated through a single anti-V5 immunoprecipitation step so as to preserve weak interactions (middle and right gels, Fig. 2a), and the proteins analyzed by tandem mass spectrometry (MS/MS). Compared with the negative (untagged) control, the NCU09482 (BRD-8)-interactome is highly enriched for subunits of the NuA4 histone acetyltransferase complex (Fig. 2b) (Supplementary Data 1). Unlike other subunits of NuA4 that have no peptides recovered from the negative
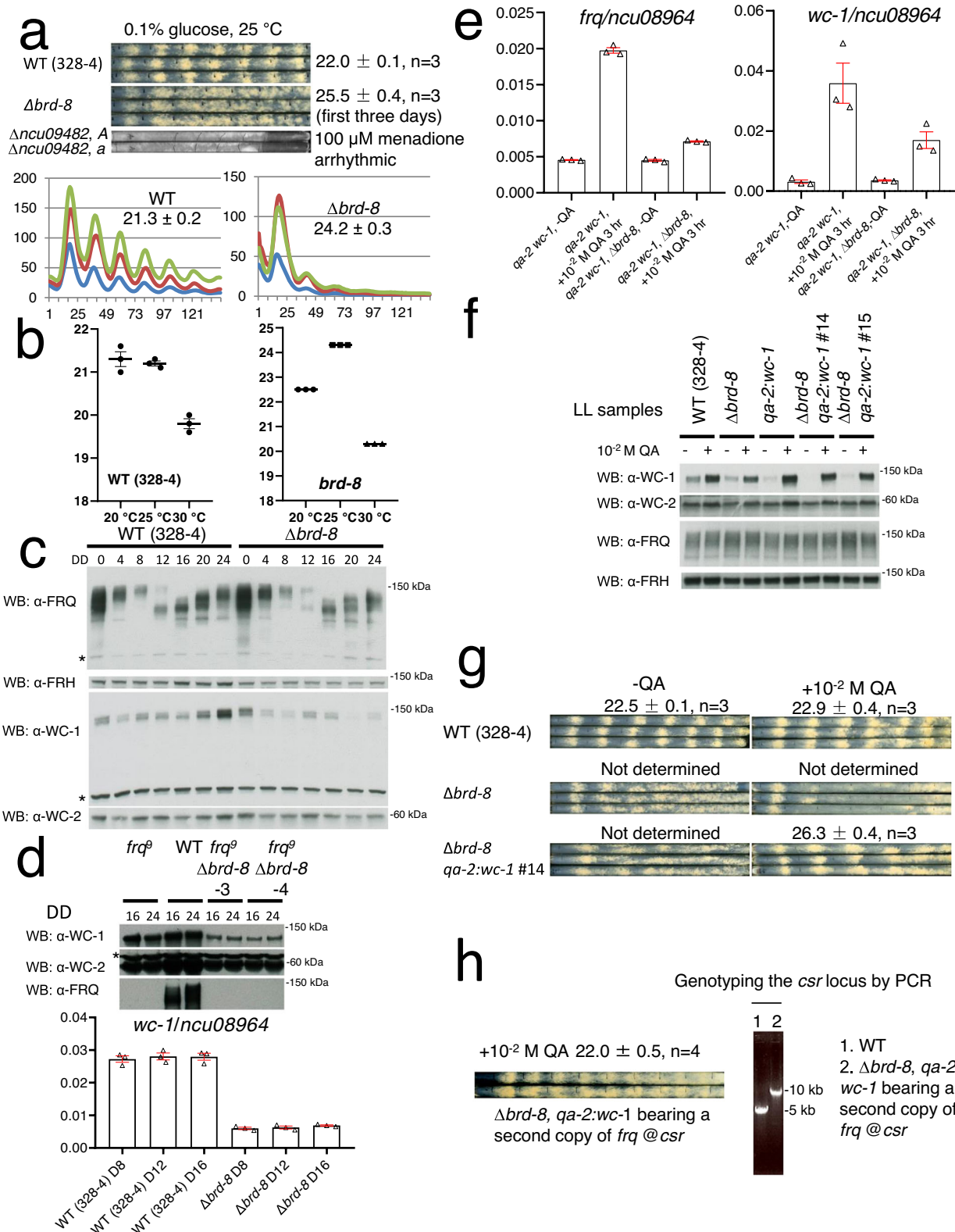
control (WT [untagged] in Fig. 2b), Arp4 itself seems a sticky protein with respect to the affinity resin, similar to actin in the same figure. In *Neurospora*, Arp4 may not exist only in the NuA4 complex but may also be present as an abundant noncomplexed protein that can bind to the antibody-conjugated resin in a nonspecific manner. To verify these interactions in vivo, NCU09482 (BRD-8) was C-terminally tagged with V5 or VHF, while BYE-1 and most NuA4 subunits including VID-21, EAF-

6, EAF-3, YAF-9, EAF-7, ESA-1 etc. (Fig. 2c), were individually tagged with 3 x FLAG or V5. Immunoprecipitation using V5 or FLAG antibody confirmed the interaction between BRD-8 and all NuA4 subunits as well as BYE-1 in vivo (Fig. 2c). NGF-1, a histone H3 acetyltransferase and the ortholog of Saccharomyces GCN5, was chosen as a control to prove the specificity of interactions between BRD-8 and its interactors. No interaction was detected between BRD-8 and NGF-1 (Supplementary

Fig. 1 | Identification of *brd-8* as a regulator of the *Neurospora* core circadian oscillator and output. Δ*brd-8* was assayed by race tube (**a**, upper) and luciferase (**a**, lower) analyses. Of the race tube analyses, only Δ*ncu09482, a* and Δ*ncu09482, A* were grown on regular race tube medium containing 100 μM menadione and showed an arrhythmic overt clock. **b** Circadian periods of WT and Δ*brd-8* at 20°, 25°, and 30 °C were determined by the luciferase assay. The period data presented here are the average +/- the standard error of the mean (SEM). Raw data are shown in Supplementary Figure 2. **c** Expression of FRQ, FRH, WC-1, and WC-2 in WT and Δ*brd-8* over 24 hr. DD, hours after the light to dark transfer. The experiment was repeated three times with similar results. **d** Upper panel, total WC-1, WC-2, and FRQ were followed by Western blotting at DD16 and DD24 in WT, *frq⁹*, and *frq⁹*; Δ*brd-8*. Lower panel, mRNAs extracted from samples cultured in the dark for 8, 12, and 16 h. **e** Expression of *wc-1* and *frq* in *qa-2:wc-1* and *qa-2:wc-1*; Δ*brd-8* was determined by RT-qPCR in the absence or presence of 10^{-2} M quinic acid (QA) for 3 hrs. In Fig. 1d and e, the RT-qPCR data are representatives of three biological experiments (n = 3) and reported as the average +/- SEM; gene expression was normalized to that of *ncu08964*. **f** Total WC-1, WC-2, FRQ, and FRH were measured in WT, Δ*brd-8*, *qa-2:wc-1*, and *qa-2 wc-1*; Δ*brd-8* with or without QA in the medium as indicated. The experiment was done three times, and similar results were obtained. **g** Race tube analyses of WT, Δ*brd-8*, and Δ*brd-8*; *qa-2:wc-1* in the absence or presence of 10^{-2} M QA. **h** Knocking in a second copy of *frq* at the *csr* locus rescues the long period length observed in Δ*brd-8*. The amplicon with a primer set used in genotyping is against the *csr* locus; in the *frq* knock-in strain, a PCR product with a larger size was amplified by PCR compared to that in the WT. Source data are provided as a Source Data file.

Fig. 4a), indicating the interaction between BRD-8 and NuA4 subunits is not through promiscuous binding with whole chromatin; from the interactor list identified with BRD-8^V5 (Supplementary Data 1), fatty acid synthase beta subunit (CEL-2) and HSP-70-5 (HSP70-like) were selected as controls to validate the mass spectrometry result, and their interactions with BRD-8 were also not seen (Supplementary Fig. 4b, c). Because *Neurospora* is an ascomycete fungus, BLASTP was used to search for orthologs to the protein encoded by NCU09482 among fungi; surprisingly no orthologs were detected in Saccharomyces or *S. pombe* although outside of these groups and within the Pezizomycotina, the protein encoded by NCU09482 was found to be well conserved (Supplementary Fig. 5). However, NuA4 subunits have not been previously described among these organisms, so the search for orthologs was extended to animals. Interestingly, the top BLASTP hit in humans is BRD8, a component of the animal NuA4 complex not previously found in fungi[49], and reciprocally BLASTP of the *Neurospora* proteome using human BRD8 identifies the protein encoded by NCU09482 as the next to top hit. Because the protein encoded by NCU09482 specifically associates with NuA4 complex subunits, has a bromodomain, and shows reciprocal (close to) best homology with BRD8, in keeping with prior nomenclature precedents (e.g.[50]), it is designated as BRD-8 (bromodomain protein-8).

If loss of BRD-8 impacts NuA4 function leading to period lengthening, then loss of other NuA4 subunits or associated proteins might be expected to have similar and additive effects. This was tested; Δ*eaf-3* shows an impaired long-period core clock by a luciferase assay (Fig. 2d) and a strong growth defect by race tube analysis (Fig. 2e). Δ*bye-1* similarly displays a circadian period lengthened by ~2 hrs (Fig. 2e), while disruption of both *eaf-3* and *bye-1* leads to low and arrhythmic luciferase signals (Fig. 2d). The Δ*brd-8, Δbye-1* strain bearing deletions in both components shows a period lengthened to the same degree as the single mutants consistent with them working through the same pathway (Fig. 2d). Interestingly, in the perithecia, transcripts of all NuA4 subunits as well as BYE-1 are subject to multiple A-to-I editing events (Fig. 2b)[51]. This is of potential interest because, whereas most editing sites in animals occur in noncoding regions associated with repetitive elements, editing in fungi is typically nonsynonymous, is under positive selection, and can often lead to changes in coding or STOP sites[52].
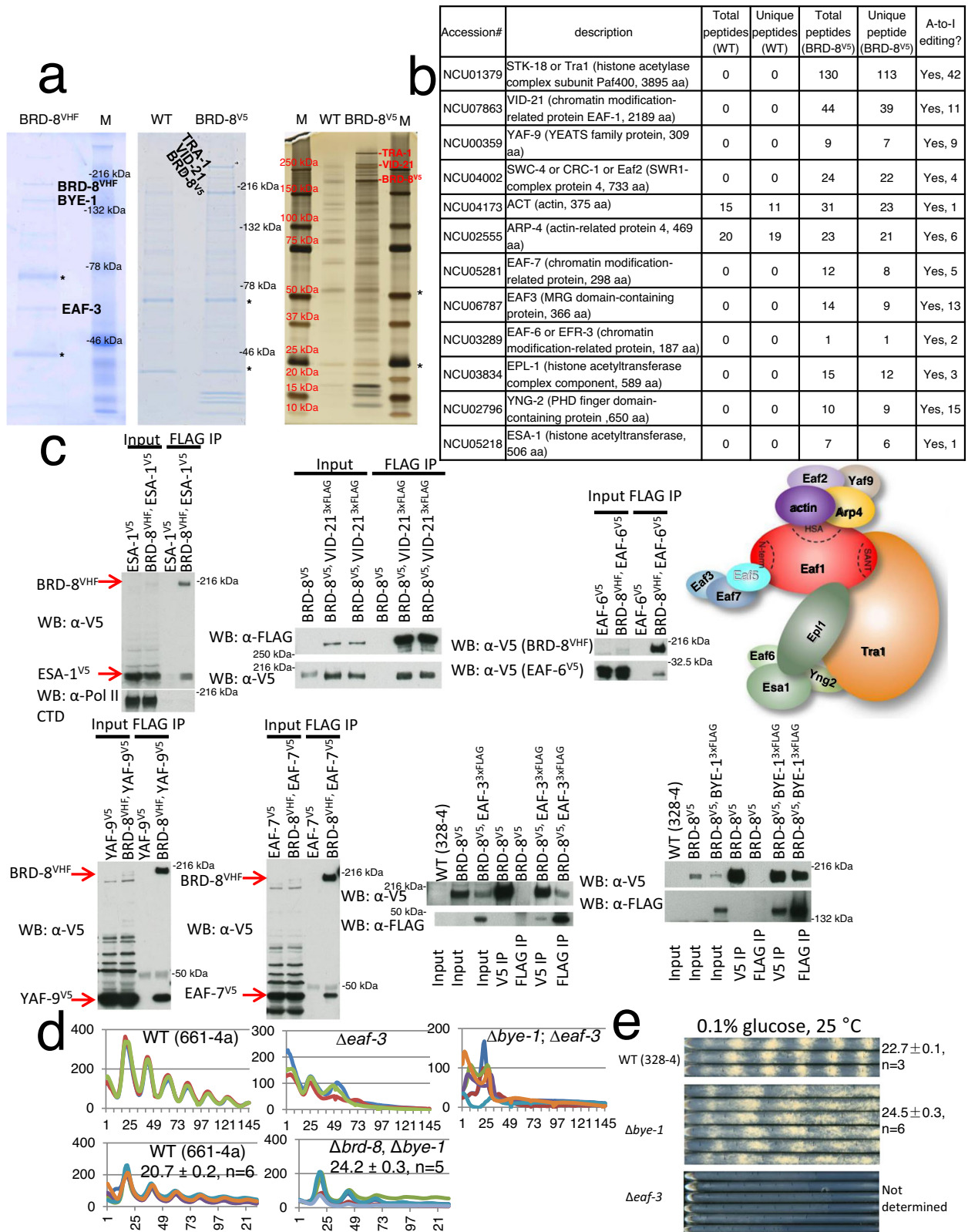
Down-regulation of *esa-1* impairs the clock

ESA-1 is the catalytic subunit of the NuA4 complex. We were unable to obtain any homokaryotic deletions of the *Neurospora* ortholog of *esa-1* (NCU05218), indicating that it is an essential gene as it is in yeast[16]. To confirm its requirement for normal rhythmicity, a construct bearing a hairpin structure specific for *esa-1* and driven by the *qa-2* promoter (inducible by QA) was transformed into an ESA-1^V5 strain, targeting the *csr* locus to create a *ds esa-1* strain affording regulatable knock-down of *esa-1*; circadian rhythms of this strain were monitored using a luciferase assay in the presence or absence of 10^{-2} M QA. In the absence of QA, the *ds esa-1* strain exhibited a robust rhythm similar to that seen in WT

(Fig. 3a). When 10^{-2} M QA was included in the medium, the robustness of luciferase signals derived from the *frq C-box* was severely impaired (Fig. 3a), consistent with ESA-1 being a histone acetyltransferase required for a normal circadian clock. To test whether disruption of ESA-1 can cause a period defect, a dominant-negative mutant of *esa-1* (*esa-1^E395Q*)[53] was knocked into a strain bearing *frq*-promoter-driven luciferase at the *his-3* locus. By adding QA, the period in *qa-2*-driven *esa-1^E395Q* is extended by ~2 hrs compared with that cultured in the QA-free medium as a control (Fig. 3a), suggesting that reduced NuA4 activity can result in a period change; Western blotting confirmed that addition of QA led to a dramatic reduction of ESA-1^V5 protein only in the *ds esa-1* strain (Fig. 3b). To test whether *Neurospora* ESA-1 can acetylate histones H4 and H2A, ESA-1^V5 was affinity-purified and tested in an in vitro acetylation assay using recombinant histones H4 and H2A. ESA-1^V5 strongly modified histones H4 at lysines 5, 8, 12, and 16 and H2A at lysine 9 (Fig. 3c). To directly test whether BRD-8 enhances ESA-1 activity, we used nucleosome core particles (NCPs) as substrate to test the importance of BRD-8, and in vitro acetylation assays were carried out with ESA-1^V5 immunoprecipitated from WT or the Δ*brd-8* background. Surprisingly, we did not see a different activity of ESA-1 in the presence or absence of Δ*brd-8* in the in vitro acetylation assay (Fig. 3c), which suggests either that Δ*brd-8* might regulate the nucleosomal accessibility of NuA4 in vivo and that free histones used in the in vitro acetylation assays could not fully recapitulate the chromatin context in vivo, or that there is more than one ESA-1-containing complex and that not all ESA-1-containing complexes contain and are regulated by BRD-8.

brd-8 is required for normal histone H4 acetylation and Pol II binding at the promoter and coding region of *frq*

To examine how *brd-8* influences histone H4 and its acetylation status in vivo, H4 and acetyl H4 were analyzed by chromatin immunoprecipitation (ChIP) in cultures from the late subjective night. Interestingly, histone H4 densities in Δ*brd-8* increase modestly, while the level of acetylated H4 decreases significantly at *frq, frh, wc-1, wc-2*, and other clock- and light-response-associated genes in Δ*brd-8* (Fig. 4a and Supplementary Data 2). All these data are consistent with the expected activity of BRD-8, as a NuA4 subunit, in regulating nucleosomal density and histone H4 acetylation genome-wide. Given that BRD-8 interacts with NuA4 subunits, as well as with BYE-1 (Fig. 2), a unifying mechanistic model posits that BRD-8 influences the clock through the action of NuA4 and BYE-1 on *frq* transcription. To validate the ChIP-sequencing result of *frq* in Fig. 4a, an independent ChIP experiment with new cultures was carried out in the same way as in Fig. 4a with the exception of subsequent quantitative PCRs (qPCRs) with *frq*-specific primer sets in place of DNA sequencing. The ChIP-qPCR results agree in general with the ChIP-sequencing data shown in Fig. 4a: The pan-histone H4 level at the *frq* gene was increased by approximately twofold, while that of acetylated histone H4 dropped sharply at most sites on *frq* that were examined (Supplementary Figure 6). In a third biological replicate, ChIP-qPCR assays were performed to measure the level of pan-

a

BRD-8^VHF   M   WT   BRD-8^V5   M   WT BRD-8^V5 M

TRA-1
VID-21
BRD-8^V5

BRD-8^VHF
BYE-1

EAF-3

b

Accession#	description	Total peptides (WT)	Unique peptides (WT)	Total peptides (BRD-8^V5)	Unique peptide (BRD-8^V5)	A-to-I editing?
NCU01379	STK-18 or Tra1 (histone acetylase complex subunit Paf400, 3895 aa)	0	0	130	113	Yes, 42
NCU07863	VID-21 (chromatin modification-related protein EAF-1, 2189 aa)	0	0	44	39	Yes, 11
NCU00359	YAF-9 (YEATS family protein, 309 aa)	0	0	9	7	Yes, 9
NCU04002	SWC-4 or CRC-1 or Eaf2 (SWR1-complex protein 4, 733 aa)	0	0	24	22	Yes, 4
NCU04173	ACT (actin, 375 aa)	15	11	31	23	Yes, 1
NCU02555	ARP-4 (actin-related protein 4, 469 aa)	20	19	23	21	Yes, 6
NCU05281	EAF-7 (chromatin modification-related protein, 298 aa)	0	0	12	8	Yes, 5
NCU06787	EAF3 (MRG domain-containing protein, 366 aa)	0	0	14	9	Yes, 13
NCU03289	EAF-6 or EFR-3 (chromatin modification-related protein, 187 aa)	0	0	1	1	Yes, 2
NCU03834	EPL-1 (histone acetyltransferase complex component, 589 aa)	0	0	15	12	Yes, 3
NCU02796	YNG-2 (PHD finger domain-containing protein ,650 aa)	0	0	10	9	Yes, 15
NCU05218	ESA-1 (histone acetyltransferase, 506 aa)	0	0	7	6	Yes, 1

c

WB: α-V5 (BRD-8^VHF)
WB: α-V5 (EAF-6^V5)
WB: α-FLAG
WB: α-V5
WB: α-Pol II CTD

d

e

0.1% glucose, 25 °C

WT (328-4)   22.7±0.1, n=3
Δbye-1   24.5±0.3, n=6
Δeaf-3   Not determined

and acetyl-histone H4 and Pol II at *frq* (Fig. 4b–d) at a time corresponding to mid-subjective-morning, the peak of *frq* transcription (DD16 in WT and DD19 in Δ*brd-8*). Consistent with results from ChIP-sequencing (Fig. 4a), histone H4 levels at *frq* in Δ*brd-8* were slightly higher than those in WT (Fig. 4b), whereas the levels of acetyl histone H4 are significantly lower in Δ*brd-8* than WT (Fig. 4c), and Pol II density within *frq* in Δ*brd-8* is ~50% than in WT (Fig. 4d). The level of

WC-1 is lower in Δ*brd-8* (Fig. 1) so the reduced levels of histone acetylation and Pol II might be caused by decreased WCC binding to the *frq* promoter. To address this question, ChIP assays were performed using a strain in which *wc-1* driven by the *qa-2* promoter is over-expressed in Δ*brd-8* (Fig. 1f, g). Interestingly, although WC-1 over-expression in Δ*brd-8* resulted in an even slightly higher binding of WCC to the promoter region of *frq* (Fig. 4e) and in lowered histone H4 at *frq* (Fig. 4f),

Fig. 2 | BRD-8 interacts with NuA4 subunits and BYE-1. a Coomassie blue- and silver-stained gels showing BRD-8^{VHF} or BRD-8^{V5} and its interactome purified from a culture grown in the light. BRD-8 and interactors were affinity-purified, run on SDS-PAGE gels, and analyzed by mass spectrometry. For the BRD-8^{VHF} interactors (left gel, purified from 30 g of tissue grown in the light by tandem V5, His, and FLAG steps), individual interactor bands were removed for mass spectrometry analyses, while for BRD-8^{V5} (middle and right gels, each purified from 5 g of tissue grown in the light by a single V5 step), either individual bands or the whole interactome (the entire Coomassie blue-stained gel lane; see Methods) was removed and then analyzed. The rightmost gel was loaded with extracts equivalent to the middle gel but was silver-stained to afford greater sensitivity in visualizing protein bands. Purification with BRD-8^{VHF} was done twice and similar results were seen; interactor identification from BRD-8^{V5} was performed three times, and similar band profiles were observed. **b** List of NuA4 subunits interacting with BRD-8^{V5} identified by mass spectrometry (See Supplementary Data 1 for the full list of BRD-8^{V5} interactors identified). The number of A-to-I editing events on these NuA4 subunits (retrieved from[51]) are also shown in the table. Annotations for the genes were obtained from FungiDB (https://fungidb.org/fungidb/app) and Uniprot (https://www.uniprot.org/). **c** Verification of interaction between BRD-8 and NuA4 subunits by co-immunoprecipitation. All epitope tags were added to genes at their native loci except for *eaf-3*^{3xFLAG}, that was targeted at the *csr* locus. The schematic architecture of *Saccharomyces cerevisiae* NuA4 was modified from (Wang, X., Ahmad, S., Zhang, Z. et al. Architecture of the *Saccharomyces cerevisiae* NuA4/TIP60 complex. *Nat Commun* 9, 1147 [2018]. https://doi.org/10.1038/s41467-018-03504-5)[97] with EAF5 dimmed to indicate that it was not found in our extracts. These experiments were carried out three times, and results were similar. **d** Bioluminescent analyses of *frq C-box* activity in WT, Δ*eaf-3*, and Δ*eaf-3*; Δ*bye-1* at 25 °C by the luciferase assay. **e** Race tube analyses of WT, Δ*eaf-3*, and Δ*bye-1*. Source data can be found in the Source Data file.

the levels of acetylated histone H4 (Fig. 4g) and Pol II (Fig. 4h) are still much lower than those in WT, suggesting that BRD-8 positively regulates ESA-1 function in vivo independent of WCC. ChIP-qPCR assays revealed that at DD16, when *frq* transcription is high, BRD-8 associates with both cis-acting elements in the *frq* promoter (*C-box* and *pLRE*) as well as the coding region of *frq* (Fig. 4i, j). Interestingly, the binding of BRD-8 to the *frq* gene is not dependent on the level of WC-1 expression (Fig. 4i, j), suggesting that the recruitment of BRD-8 to *frq* does not rely on active transcription.

Structure-function analysis of the NuA4/BRD-8/BYE-1 complex identifies regions of BRD-8 required for BYE-1 and ESA-1 interaction

To determine whether BRD-8, BYE-1, and NuA4 are in the same or different complexes, BRD-8, BYE-1, and ESA-1 were tagged with V5, 3 x HA, and 3 x FLAG, respectively. Immunoprecipitation with FLAG antibody-conjugated resin was performed, the complex was eluted with 3 x FLAG peptide, and then the ESA-1-3 x FLAG peptide elution was re-immunoprecipitated with V5 antibody. Interestingly, BRD-8, ESA-1, and BYE-1 were seen in the same complex despite a relatively low level compared with inputs (Fig. 5a), suggesting that they might have a functional overlap. However, in strains lacking BRD-8, BYE-1 no longer interacts with ESA-1, indicating that BRD-8 is required to bridge this interaction and bring BYE-1 into the complex (Fig. 5b). To test whether ESA-1 and BRD-8 associate with each other quantitatively, immuno-depletion assays were performed using cultures grown in constant light. Immunodepletion of BRD-8^{V5} with V5 antibody only pulled down a fraction of ESA-1 (Fig. 5c left), suggesting that different pools of NuA4 complexes exist in the cell. Immunodepletion of ESA-1$^{3 x FLAG}$ with FLAG antibody pulled down all BRD-8^{V5} molecules (Fig. 5c right), suggesting that all BRD-8^{V5} is complexed with NuA4 in the cell. These data explain the results of the in vitro histone acetylation assays (Fig. 3c), and are consistent with a model in which BRD-8 can modulate the activity of some but not all NuA4 activity in the cell, and may be reminiscent of recent reports that human BRD8 participates in multiple complexes[54]. When *Neurospora* BRD-8^{V5} and BYE-1, ARP-4, or EPL-1 were co-expressed in *E. coli*, an interaction was detected by immunoprecipitation (Supplementary Fig. 7), indicating that BRD-8 directly associates with NuA4 subunits and BYE-1. BRD-8 is widely conserved among the ascomycete fungi as noted above, indeed more so as compared to a NuA4 subunit described in Saccharomyces but not found in *Neurospora*, EAF5, whose orthologs are restricted to Saccharomyces and closely related species (Supplementary Fig. 5). Indeed there is strong evidence suggesting that human BRD8 is the functional homolog of yeast EAF-5, acting as a bridge protein in some complexes[54].

To identify motifs in BRD-8 essential for its circadian function and intra-complex interactions, strains bearing a series of deletions of *brd-8* (Fig. 5d) were generated and analyzed by race tube and Western blotting assays. Western blotting analyses showed that of the four

brd-8 deletion strains, only Δ1030-1306 has a reduced protein level (Supplementary Figure 4d). Two of these mutants, missing aa 2–348 and aa 703-1029, showed a conidiation phenotype similar to Δ*brd-8* (Fig. 5e), suggesting that these two regions are required for its circadian function. Although analysis of BRD-8's open reading frame (ORF) revealed a region of bromodomain near the C-terminus of the protein (Fig. 5d), deletion of aa 1030–1306 within which the bromodomain is located resulted only in a slightly longer period (23.4 hrs) (Fig. 5e, f), which suggested that the domain is not essential for its circadian function. This result is consistent with the existence of multiple BRD-8-containing complexes in the cell, only some of which require the bromodomain, and that those requiring the bromodomain are not the functions relevant to circadian timekeeping.

Because ESA-1 and BYE-1 were identified from the BRD-8 interactome analyses and disruption of either gene results in a lengthened circadian period, we checked by immunoprecipitation whether the interaction between BRD-8 and ESA-1 or BYE-1 is influenced in the *brd-8* mutants. Interestingly, BRD-8$^{Δ2-348}$, in which a proline-rich low complexity region is deleted, binds normally to BYE-1 but does not interact with ESA-1 (Fig. 5g), while BRD-8$^{Δ703-1029}$ associates with ESA-1 but fails to complex with BYE-1 (Fig. 5h), consistent with BRD-8 being the adapter protein for ESA-1 and BYE-1. *brd-8*$^{Δ349-702}$ and *brd-8*$^{Δ1030-1306}$ showed normal interactions with ESA-1 and BYE-1 (Fig. 5g, h) and displayed ~WT circadian phenotypes (Fig. 5e, f).

Characterization of roles for BRD-8 in the circadian system

To directly test whether there is a causality between the level of *brd-8* and circadian periods, we made a strain in which the ORF of *brd-8* is under the control of the quinic acid-inducible promoter (*qa-2*) at its native locus. In the presence of QA, the controlled gene is constitutively induced by the *qa–2* promoter. Interestingly, the level of *brd-8* positively correlated with shortening of the period of the circadian conidiation rhythm within a certain range of QA concentration (10^{-5} to 10^{-3} M) (Fig. 6a, b, and c); however, when the QA concentration reaches 10^{-2} M, the period is slightly lengthened (Fig. 6a–c), which might be caused by the indirect effect of the high BRD-8 level on the expression of other proteins that might indirectly influence the circadian clock. The level of BRD-8 is higher when cultured in 2% glucose LCM than in 0.1% LCM, while the ESA-1 level is constant in 2% vs 0.1% glucose LCM (Fig. 6d). The BRD-8 level is significantly lower than that of ESA-1 (Fig. 6d and supplementary figure 8a), consistent with the immunoprecipitation data of Fig. 5b, c. The BRD-8 protein was highly enriched in the nucleus (Fig. 6e), consistent with its role in regulating transcription. BRD-8 does not interact with itself (Supplementary Fig. 4e), suggesting that NuA4/BRD-8/BYE-1 does not form an oligomer, and BRD-8 might only exist in the NuA4 complex.

Because the circadian clock in *Neurospora* globally regulates gene expression, we investigated whether the expression of BRD-8, BYE-1, and several additional NuA4 subunits are also under circadian control.
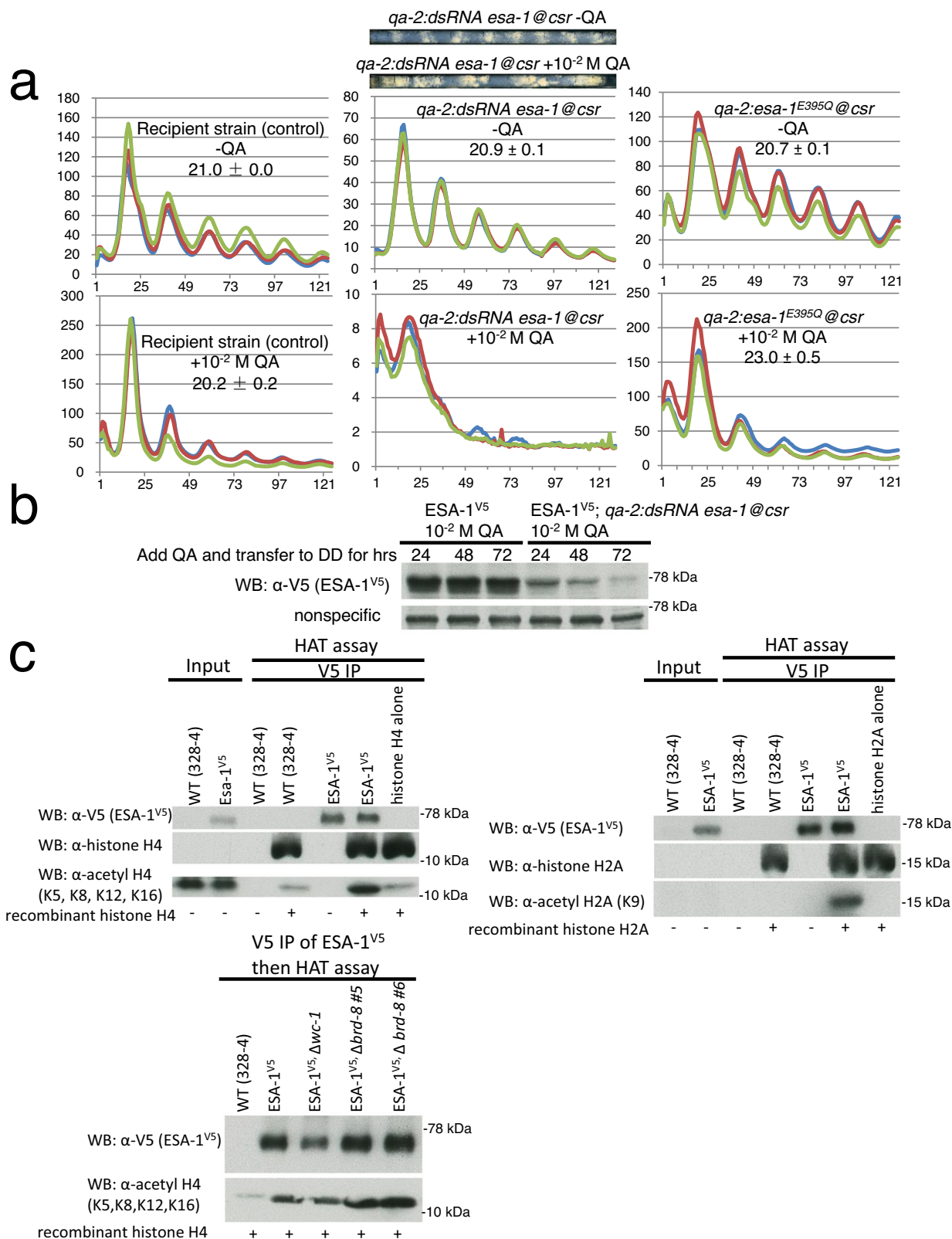
Promoters of *brd-8*, *bye-1*, *eaf-3*, *vid-21*, and *esa-1*, along with *histone h2a.z*, and *histone h4-1* were fused with the codon-optimized LUC gene respectively and transformed to the WT strain at the *csr* locus. The promoters of *brd-8*, *bye-1*, *eaf-3*, *vid-21*, and *histone h2a.z* genes were shown to drive rhythms in LUC expression (Fig. 6f), and ARP-4 was found to be rhythmic in a separate study[55], while no obvious circadian rhythmicity was seen for the *esa-1* or *histone h4-1* promoter

(Supplementary Fig. 8b). Furthermore, to better understand and analyze *brd-8* dynamics in vivo, we constructed a *brd-8*-luciferase translational fusion reporter that directly tracks BRD-8 protein expression and transformed it into the WT strain. The protein level of BRD-8-LUC oscillated in vivo in a circadian manner (Fig. 6f), confirming that *brd-8* is a *ccg* (*clock-controlled gene*), and the strain bearing BRD-8-LUC showed an overt rhythm with a WT period (Fig. 6g), indicating that LUC

Fig. 3 | *esa-1* knockdown causes a long period. a Bioluminescent analysis of strains that knock down *esa-1* (middle) or overexpress *esa-1^{E395Q}* (right). *qa-2*-driven double-stranded RNA against *esa-1*, or *esa-1^{E395Q}* targeting the *csr* locus, was transformed to a WT strain. Circadian periods of WT and Δ*brd-8* at 25 °C were determined by the luciferase assay in the absence or presence of 10^{-2} M QA as indicated. Race tube images on the top indicate the viability of the *qa-2*-driven double-stranded RNA against *esa-1* strain grown with 10^{-2} M QA despite a slow and unstable growth rate compared with the no QA control. **b** *qa-2:dsRNA* against *esa-1* was transformed to *esa-1^{V5}*; strains were cultured in constant light, and 10^{-2} M QA was added to the cultures and immediately transferred to the dark for 24, 47, and 72 hrs; Western blotting against V5 was performed and a non-specific band was shown for equal

loadings. The assay was performed three times, and similar results were observed. **c** In vitro HAT assays of recombinant histone H4 (upper left) or H2A (upper right) with affinity-purified ESA-1^{V5}. Details for this assay are described in Methods. Bottom, a HAT assay of ESA-1^{V5} in vitro. ESA-1^{V5} in the background of WT, Δ*wc-1*, or Δ*brd-8* was immunoprecipitated by V5 antibody and assayed in vitro with recombinant histone H4 to test its histone acetylation activity. Western blotting using antibodies against V5, acetyl histone H2A (K9), and acetyl histone H4 (K5, K8, K12, and K16) respectively were followed to show ESA-1^{V5} and acetylated histone H2A and H4 levels. The assay was done three times with similar results. Source data were deposited in the Source Data file.

does not impact its function. The data are consistent with a model in which an BRD-8/BYE-1/NuA4 complex controls *frq* expression and thereby the clock, perhaps by modulating transcription elongation, while several subunits of the BRD-8/BYE-1/NuA4 complex are also themselves under circadian control. In this way, elements of the BRD-8/BYE-1/NuA4 complex both regulate the clock and are regulated by the clock, contributing to a feedback loop surrounding the core circadian oscillator.

Inhibition of CDK-9 further lengthens the circadian period of Δ*brd-8*

If mutations in the NuA4/BRD-8/BYE-1 complex impact the clock by affecting transcription elongation, then other mutations or chemicals impacting elongation should have similar effects on the clock and, importantly, loss of BRD-8 might be expected to sensitize the clock to treatments affecting elongation. Phosphorylation of Ser2 in the Pol II C-terminal domain (CTD) is required for Pol II elongation processivity, and CDK-9 (SGV1 in Saccharomyces) is the kinase phosphorylating Ser2. To test whether inhibition of CDK-9 causes a period effect on Δ*brd-8*, strains were grown on medium containing different concentrations of AZD4573[56–59], a highly specific CDK-9 inhibitor, and circadian oscillations were monitored by luciferase assays. A clear trend of period lengthening effects was observed in WT in the presence of 1–100 μM AZD4573, while Δ*brd-8* shows even a stronger dose effect on period changes than WT, especially 100 μM at which concentration Δ*brd-8* becomes completely arrhythmic, while WT is ~ 6 h longer than seen under no drug treatment (Fig. 7a). CDK-9 was also downregulated independently by replacing its native promoter with the *qa-2* promoter; luciferase assays were conducted in the absence of QA. Compared with Δ*brd-8* (Fig. 7a), Δ*brd-8, qa-2:cdk-9* displays a further lengthened period by 2-3 hrs (Fig. 7b). The data suggest that the absence of *brd-8* makes Pol II more susceptible to inhibition, and both chromatin architecture and robust Pol II elongation are required for the period-length determination.

Discussion

The *frequency* gene encodes the central scaffold protein that organizes the negative arm repressive complex in the *Neurospora* clock, playing the same role in *Neurospora* as that ascribed to the PER proteins in the mammalian clock; as a result, its expression is carefully regulated. *frq* is rhythmically transcribed and translated in the dark[10], a result of chromatin remodelers and modifiers that co-execute their effects at the *frq* locus, and most research on its transcriptional regulation has focused on transcription initiation at the *C-box* rather than on steps in transcription elongation. During daylight the *frq* gene lies in a region largely free of nucleosomes and showing rapid nucleosome turnover[11], and in the dark several distinct chromatin remodeling complexes have been identified in controlling *frq* expression, including CSW (Clockswitch)[60], CHD1 (chromodomain helicase DNA–binding)[61], SWI/SNF (SWItch/Sucrose NonFermentable)[62], CLOCK ATPase (CATP)[63], Centromere Binding Factor 1 (CBF-1)[64], and IEC-1-INO80 complex[65]. Histone modifications can also lead to changes in gene expression, especially methylation and acetylation of N-terminal tails of histones which are

known to influence condensation as well as serving to call down modifiers[66–69]; indeed one study has reported that the lysine methyltransferase SET1 is required for methylation of lysine 4 of histone H3 and normal circadian expression of *frq*[70]. Here, by a circuitous route beginning with an unbiased genetic screen, we have identified a phylogenetically conserved auxiliary subunit of the canonical NuA4 histone acetyltransferase complex and shown that it also complexes with elements involved in transcription elongation, and that in the aggregate mutations in these elements impact *frq* expression and the progress of the circadian clock. In the process, we also discovered that there are multiple NuA4 complexes, presumably with altered activities, and that some include an ortholog of the regulator of transcription elongation, BYE-1, first described in Saccharomyces[24] but with orthologs in humans[26]. Genetic and pharmacological data are consistent with a model in which the NuA4 complex that includes BRD-8 and BYE-1, but not the canonical complex, is involved in controlling *frq* expression in the service of the clock (Fig. 7c). Given that the expression of a number of NuA4 subunits is in turn regulated by the clock, it seems likely that events surrounding histone acetylation and transcription elongation describe a feedback loop surrounding the core clock.

This work follows the lines of Belden, He, Liu, and others[60–64] showing that normal transcription of *frq* is required for normal clock function, and also the thorough study of Petkau et al.[23] which revealed a role for Pol II pause/release and transcription elongation in the mammalian clock. In this way, analysis of circadian rhythmicity provides an especially sensitive tool for dissection of transcriptional regulators because differences in period length are biologically meaningful, more nuanced than life/death (e.g. identification of essential genes) and can be reliably measured with precision of +/− 10%. The BRD-8-containing NuA4 complex however, like the other chromatin-regulating and clock-affecting complexes, would not be considered a core clock component because its role in rhythmicity is solely conferred by its action on *frq* expression whose rhythmicity is driven through WCC, and the rhythm persists in the absence of BRD-8; instead these are all clock-affecting. This said, the data do show that not all genes are bound by nor their expression influenced by complexes that contain BRD-8 and BYE-1. Instead action of these NuA4-associated factors is restricted, although they do appear to be quite important when present: Data shown in Figs. 5c and 6d suggest that BRD-8 only accounts for a small fraction of ESA-1-containing NuA4 complexes, but deletion of *brd-8* resulted in ~50% reduction of histone H4 acetylation at the *frq* locus, suggesting a higher activity of the BRD-8-containing NuA4 complex.

Composition of NuA4 complexes

In this study several subunits associating with the NuA4 complex were identified including BRD-8 and BYE-1 (Fig. 7c). In yeast, the NuA4 complex is comprised of 13 subunits (Fig. 2c). In *Neurospora*, however, no gene having homology to *eaf-5* exists, and indeed orthologs of EAF5 are found only in Saccharomyces and closely related species (Supplementary Fig. 5). Among the aspects of physiology possessed by fungi outside of the Saccharomycotina are responses to environmental stimuli including light and time-of-day, circadian biology.
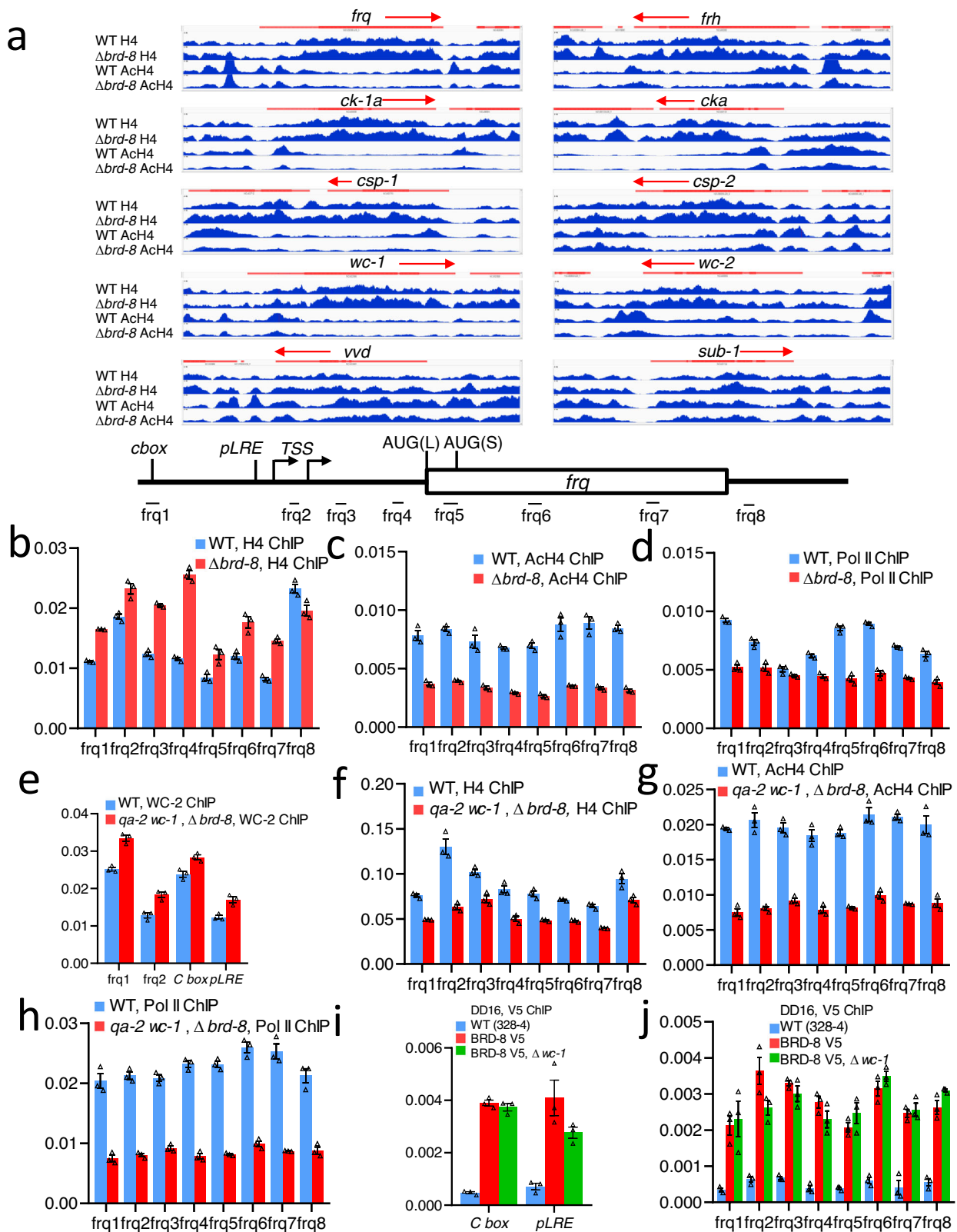
This correlation suggests the possibility that multiple NuA4 complexes with more subunits may have evolved to support additional aspects of physiology.

Another aspect of regulation found in *Neurospora* but not Saccharomyces is RNA A-to-I editing. In the fungi this mainly occurs in coding regions and results in nonsynonymous changes to proteins encoded[51], which dramatically extends the proteomic complexity during translation and thus can broadly impact cellular and physiological events. Interestingly, mRNAs of all NuA4 subunits undergo multiple A-to-I editing events in the sexual phase (Fig. 2b), which may enable histone H4 acetylation to epigenetically control the chromatin state favoring sexual development and adaptation by influencing chromatin events such as gene expression, DNA repair, and genome duplication.

Fig. 4 | Δbrd-8 has reduced acetyl-histone H4 and Pol II levels at *frq*. a The Integrative Genomics Viewer (IGV) visualization of ChIP-sequencing data. Antibodies against histone H4 or acetyl histone H4 (AcH4) were applied in ChIP experiments using cultures collected at DD20 for WT and DD26 for Δ*brd-8* to compensate the 3-h period lengthening and 3-h phase delay seen in the mutant. Only the ChIP-sequencing data are shown. Red bars represent coding regions of the genes: ORFs are in bold while UTRs or introns are in thin bars and arrows designate the direction of transcription. Bottom, diagram of the *frq* gene showing regions amplified by primer sets used in ChIP-qPCRs (Fig. 4b-J) as derived from a previous publication[94] with removal of unrelated information. To validate the data in Fig. 4a, independent *Neurospora* samples were collected in the same way as in Fig. 4a (WT at DD20 while Δ*brd-8* at DD26), and then ChIP-qPCRs were carried out using histone H4 (**b**) acetyl-histone H4 (**c**), or Pol II (**d**) antibody and *frq*-specific primer sets in (**a**)

with WT and Δ*brd-8*. In another set of biologically independent experiments (e-h) to rescue the decreased level of WC-1 in Δ*brd-8*, the promoter of *wc-1* in Δ*brd-8* was replaced by an inducible *qa-2* promoter. Two strains, WT and *qa-2* promoter-driven *wc-1* in Δ*brd-8*, were cultured in the presence of 10^{-2} M QA throughout and afterwards both harvested at DD16. **e** ChIP-qPCRs were carried out using WC-2 antibody with primers "*frq1*", "*frq2*", "*C-box*", and "*pLRE*" in WT and *qa-2:wc-1*; Δ*brd-8* at DD16. ChIP-qPCRs were performed with histone H4 (**f**), acetyl-histone H4 (**g**), or Pol II (**h**) antibody and *frq*-specific primer sets in (**a**) with WT and *qa-2:wc-1*; Δ*brd-8* at DD16. ChIP-qPCRs were done using V5 antibody with primers "*C-box*" and "*pLRE*" (**i**) and "*frq1-8*" (**j**) in WT, *brd-8ᵛ⁵*, and *brd-8ᵛ⁵*; Δ*wc-1* at DD16. For ChIP-qPCR assays, three technical replicates were performed, and the bars represent average values plotted as a percentage of the input, with error bars representing the SEM (n = 3). Source data were supplied in the Source Data file.

Dual regulation between circadian clock and basic transcriptional processes

BRD-8 influences rhythmicity through chromatin events. In Δ*brd-8*, nucleosome density is higher at *frq* while histone H4 is less acetylated than in WT, both of which effects will impede *frq* transcription. *frq* is known to lie in a region characterized by very rapid nucleosome turnover[11] so in affecting nucleosome density and modification, loss of *brd-8* might be expected to cause reduced *frq* expression and a long period which can be rescued by adding a second copy of the *frq* gene to the Δ*brd-8* strain. The data are consistent with models in which timely expression of *frq* is required for bringing kinases to phosphorylate WCC and effect repression in the circadian cycle. As FRQ and WC-1 are present in similar amounts and FRQ-promoted WCC phosphorylation is a slow process, at least in part because FRQ is predominantly cytoplasmic[9], the level of FRQ needs to be sufficient to bring about repression to WCC.

BYE1 was originally identified in Saccharomyces through a mutation that bypassed the requirement for the essential prolyl isomerase ESS1[24]. Ess1-induced conformational changes are seen as attenuating Pol II elongation, thus helping to coordinate the assembly of protein complexes on the Pol II CTD and thereby regulating transitions between multiple steps of transcription[24]. BYE1 binds directly to Pol II during early transcription elongation and tethers surrounding histones containing active post-translational modifications (PTMs), perhaps to prevent loss of histones during polymerase passage through chromatin[26] but also slowing transcription. Although in Saccharomyces BYE1 works as a free protein, its action(s) in *Neurospora* in conjunction with NuA4 may be similar to those seen in yeast, acting on elongation through regulating Pol II CTD or just enhancing ESA-1 activity on chromatin, an activity not reported in Saccharomyces. In either case, a seeming paradox in the circadian data related to loss of BRD-8 and BYE-1 arises from the facts that (1) loss of BRD-8 which results in increased nucleosome density is expected to slow transcription but (2) loss of BYE-1, a negative regulator of transcription elongation[26], would be expected to increase transcription elongation; yet both result in period lengthening. One clue to this lies in the data from Fig. 5 showing that BRD-8 forms the bridge between ESA-1 and BYE-1; hence, loss of BRD-8 results in parallel loss of BYE-1 from the NuA4 complex. This still leaves unexplained, however, how single loss of BYE-1 in the presence of normal BRD-8 results in modest period lengthening. A possible resolution to this lies in the data of Fig. 6 which detail the dosage effects of BRD-8 on rhythmicity. While complete loss of BRD-8 slows period to the greatest extent, the highest expression of BRD-8 also results in modest period lengthening, comparable to loss of BYE-1. It may be that overexpression BRD-8 has consequences on transcription similar to loss of BYE-1, and that normal rhythmicity requires a happy medium of regulators of transcription elongation, allowing it to proceed but not to proceed so quickly as to interfere with ordered assembly of protein complexes on the Pol II CTD.

BRD-8, the NuA4 complex, and roles for acetylation

The unexpected identification of a human BRD8-like protein associated with a fungal NuA4 acetyltransferase complex, and the role of acetylation in the fungal clock, warrant comment. In mammals, Brd8 is expressed in multiple isoforms, some with one and some with two bromodomains, although expression of the two-bromodomain isoform is restricted to testes, whereas the single bromodomain isoform is ubiquitously expressed (e.g., GTExportal.org) and it is similar in size to *Neurospora* BRD-8 that likewise has a single bromodomain. While as noted above, BRD8 is associated with multiple mammalian complexes including NuA4/TIP60, the association of a bromodomain-containing protein in a fungal NuA4 complex has been debated (reviewed in refs. 49,71). Bdf1 in the *Saccharomyces cerevisiae* SWR1 complex, has a single bromodomain as does Bdc1, a component of the NuA4 histone acetyltransferase complex In *Saccharomyces pombe* (reviewed in refs. 49,71). However, the overall amino acid identity of *Neurospora* BRD-8 with Bdf1 and Bdc1 is relatively low (6.96% and 3.9%, respectively, similar to background), Bdf1 and Bdc1 are a third of the size of BRD-8, and perhaps most significantly, neither Bdf1 nor Bdc1 are BLASTP hits with BRD-8. Bdf1 is, however, a component of the yeast SWR complex which contains additional components orthologous to mammalian NuA4/TIP60 components, prompting the observation that the human NuA4 complex corresponds to a near-perfect fusion of the two distinct complexes in yeast, namely NuA4 and SWR1 (Doyon and Cote, 2004). This prompted us to re-examine the mass spectrometry data (Fig. 2 and Supplementary Data 1) for presence of putative SWR complex components. No peptides from subunits exclusively in SWR (i.e. orthologs of Bdf1, Vps72, Rvb1, Rvb2) were recovered from the BRD-8ᵛ⁵ purification (Supplementary Data 1), suggesting that the presence of BRD-8 in association with NuA4 is more like that seen in mammals than the association of bromodomain-containing proteins sometimes seen in yeasts.

A second point of interest sparked by the identification of BRD-8 in association with NuA4 is the potential role of acetylation in rhythmicity. This question is nicely set up by the elegant study of Petkau et al. who showed in mammals that the NuA4/TIP60 complex acetylates BMAL1 (the ortholog of *Neurospora* WC-1), providing a docking site that brings the BRD4-P-TEFb complex to DNA-bound BMAL1, promoting release of Pol II and elongation of circadian transcripts and revealing a role for control of transcriptional elongation in the mammalian clock[23]. At first glimpse there are clear parallels to the BRD-8 story here, in particular because WC-1 has been reported to be acetylated[72]; however, the similarities weaken when examined more closely. *Neurospora* does have a Brd4 ortholog (BDP-3 encoded by NCU08423) and, unlike BRD-8, it is essential as is Brd4 in humans. The acetylation of WC-1 appears only to be important for light-regulation[72], and perhaps most importantly, the structure/function data from Fig. 5d–h plainly indicate that the bromodomain of BRD-8 is not required for its circadian function. The mass spectrometry data from Supplementary Data 1 suggest that BRD-8 may interact with a number
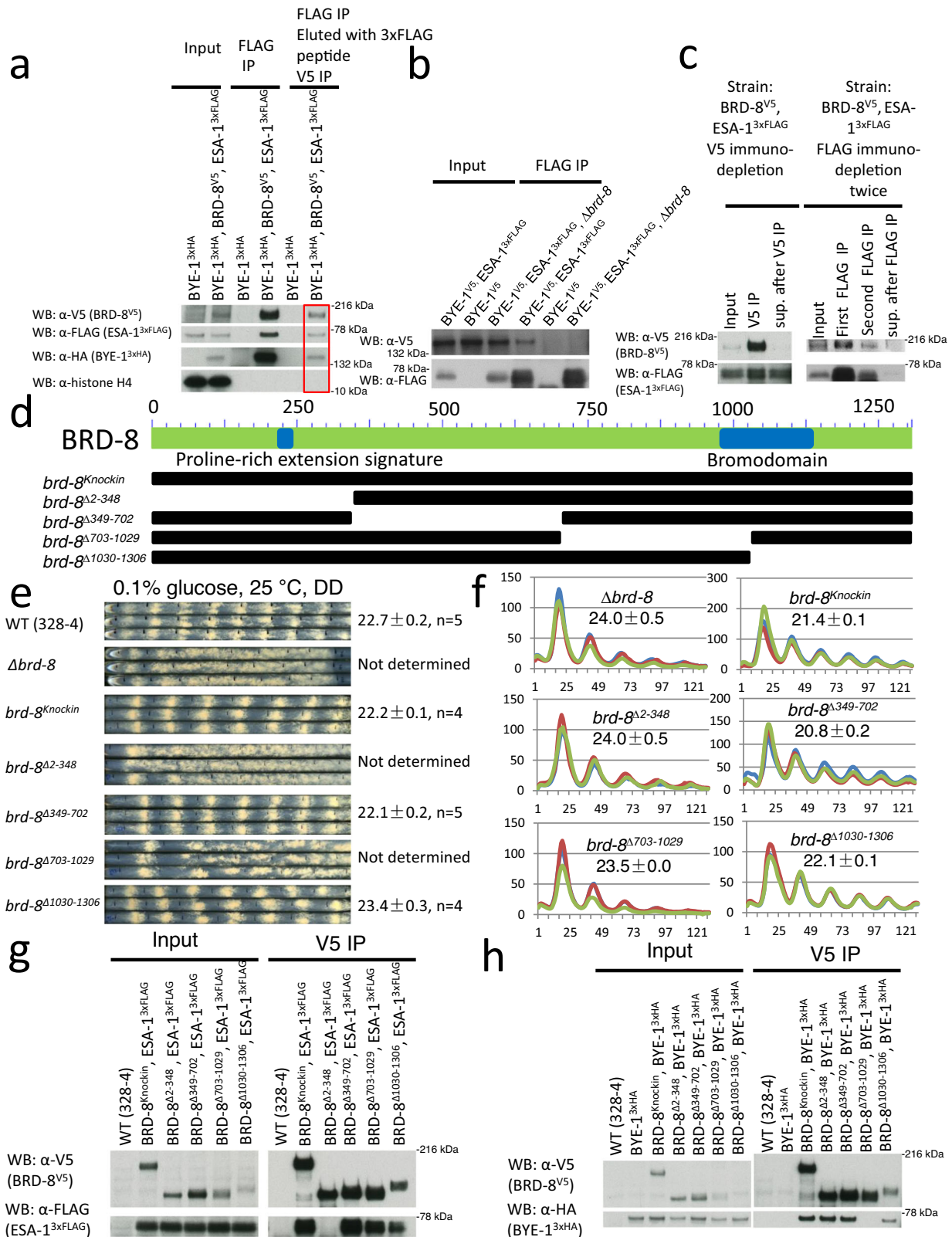
of different proteins and complexes, and if so it is like human Brd8 which interacts with at least 135 proteins (https://thebiogrid.org/116108), is ubiquitously expressed, and has roles in a host of processes; in both systems it seems plausible that not all of these roles would require the bromodomain. In the present case, BRD-8 uses its unstructured region to interact with BYE-1, and deleting its single bromodomain still results in a normal period, while removal of two

disordered domains individually phenocopies the whole gene knock-out of *brd-8* (Fig. 5d–h). Although BRD-8 provides no evidence for a role of bromodomain-mediated acetylated residue binding, a more remote route to achieve this must be mentioned. The human ortholog of BYE-1 is DIDO1 (death inducer-obliterator 1) which has been shown in a high throughput affinity capture-mass spectrometry (ms) screen[73] to interact with Brd4, the protein shown by Petkau et al.[23] to mediate

Fig. 5 | Deletion series of Δ*brd-8* identifies domains responsible for ESA-1 and BYE-1 interactions. Strains indicated were grown in constant light. **a** IP showing that fractions of BRD-8, BYE-1, and ESA-1 exist in the same complex. Protein lysate from *bye-1*[3 x HA]/*brd-8*[V5]/*esa-1*[3 x FLAG] cultured in constant light was first immunoprecipitated with FLAG-antibody resin, washed, and then eluted with 3 x FLAG peptide; for the eluate, a secondary IP was performed using V5-antibody resin; *bye-1*[3 x HA] serves as the negative control. **b** BRD-8 is required for the interaction of ESA-1 and BYE-1. IP with FLAG was performed with three strains of BYE-1[V5]/ESA-1[3 x FLAG], BYE-1[V5], and BYE-1[V5]/ESA-1[3 x FLAG]/Δ*brd-8* grown in the light. In BYE-1[V5]/ESA-1[3 x FLAG]/Δ*brd-8*, BYE-1[V5] was not detected in the "FLAG IP" lane. **c** Left, immunodepletion of BRD-8[V5] with V5 showing that not all ESA-1 molecules interact with BRD-8; right, immunodepletion of ESA-1[3 x FLAG] was done by immunoprecipitating FLAG twice and then the supernatant after the two IPs was pulled down with V5 resin, showing that all BRD-8 molecules associate with ESA-1. **d** Schematic representation of domains on BRD-8 and deletion series of *brd-8*. Race tube (**e**) and luciferase (**f**) analyses of *brd-8* deletions were performed as in prior figures (also described in Methods). **g** Immunoprecipitations using the deletion series of *brd-8* show that aa 2-348 is required for ESA-1 interaction. V5-IP followed by Western blotting against V5 and FLAG was carried out to check BRD-8[V5] and ESA-1[3 x FLAG] interaction in *brd-8* deletion series. **h** Immunoprecipitations using the deletion series of *brd-8* show that aa 703-1029 is required for ESA-1 interaction. *bye-1*[3 x HA] was targeted at the *csr* locus, while BRD-8 mutants were V5-tagged at its native loci. IP by V5 and then Western blotting with V5 and HA as indicated were carried out to check BRD-8[V5] and BYE-1[3 x HA] interaction in *brd-8* deletion series. WT (328-4, an untagged strain) serves as the negative control for IP (**g** and **h**). For **a–c**, **g**, and **h**, similar results were seen from three independent replicates. Source data are in the Source Data file.

the pause/release of Pol II from DNA-bound BMAL1. If the same mechanism worked in *Neurospora*, it should be mediated by the *Neurospora* ortholog of Brd4 (BDP-3) and be independent of the BRD-8/BYE-1 association, and if so the period lengthening seen from loss of either BRD-8 or BYE-1 alone should be additive in the double mutant Δ*brd-8*, Δ*bye-1*; however, this is not the case (Figs. 1a, and 2d). Additionally, there is no evidence (mass spectrometry in Supplementary Data 1 or targeted immunoprecipitation of BRD-8 followed by blotting for FRQ or WCC) for interaction of BRD-8 with FRQ or WCC. Lastly BDP-3 (the *Neurospora* ortholog of human BRD4) does not appear in the mass-spectrometry interactome data (Supplementary Data 1), indicating that even if BYE-1 has a circadian role through BDP-3, it cannot be linked in any mechanistic way to BRD-8.

A wealth of research in recent years has established mechanisms through which epigenetic regulation plays an important role in controlling circadian systems (reviewed in refs. [74–78]); however, the reverse has rarely been confirmed (reviewed in[79]). Here we have shown that expression of *histone h2a.z*, as well as a number of NuA4 subunits including *brd-8* gene and protein are circadianly controlled (Fig. 7c), linking the circadian clock to the basic cellular machinery. This prompted us to examine online databases for circadianly regulated genes in mammals (CIRCA: Circadian gene expression profiles; http://circadb.hogeneschlab.org) for evidence of circadian regulation of mammalian NuA4/TIP60 components. Interestingly, strong albeit sometimes low amplitude rhythms were seen for gene expression of *brd8* as well as *Trrap*, *RUVBL1*, and *DMAP1*. This suggests that in mammals, as in *Neurospora*, the events surrounding histone acetylation and transcription elongation describe a feedback loop surrounding the core clock that serves to amplify and stabilize the rhythm, contributing to persistence. These data also provide evidence for a mechanism through which the circadian clock can control gene expression through an indirect mechanism not directly mediated by the WCC or CLOCK/BMAL1 complex, the principal means of circadian output control.

Methods

Strains and growth conditions
328-4 (*ras-1*[bd], *A*) was used as a clock-WT strain in the race tube analyses and 661-4a (*ras-1*[bd], *A, his-3::C-box-driven luc*), WT in the luciferase assay; this contains the *frq C-box* fused to codon-optimized firefly *luciferase* (transcriptional fusion) at the *his-3* locus. *Neurospora* transformation was performed as previously reported[62]. To test the rhythmicity of gene expression, promoter-driven *luciferase* (*LUC*) reporter constructs were generated by transforming four PCR products [5′ of *csr*, promoter region of gene, codon optimized *luciferase* sequence, and 3′ of *csr*] with digested plasmid (*pRS426*) into yeast[80]. Race tube medium contains 1 × Vogel's salts, 0.17% arginine, 1.5% bacto-agar, and 50 ng/mL biotin with glucose at 0.1%, and liquid culture medium (LCM) contains 1 × Vogel's, 0.5% arginine, 50 ng/mL biotin, and 2% glucose. Quinic acid (QA) was added into race tube medium with certain concentrations as indicated. Unless otherwise specified, race tubes were cultured in constant light for 16–24 h at 25 °C and then transferred to the dark at 25 °C[81]. BRD-8, BYE-1, and NuA4 deletion strains generated by the *Neurospora* genome project were obtained from Fungal Genetics Stock Center (FGSC).

Protein lysate and Western blot
Procedures for preparation of protein lysates and Western blots (WB) were followed as described in refs. [8,82] For WB, 15 μgs of whole-cell protein lysate were loaded per lane in a 3-8% tris-acetate or 4-12% bistris SDS gel. Custom rabbit antibodies used in this study include antisera against WC-1 (custom antibody ordered from Pocono Rabbit Farm and Laboratory; depleted and used in Western blotting at a dilution of 1:250)[83], WC-2 (custom antibody ordered from Pocono Rabbit Farm and Laboratory; used at a dilution of 1:5,000)[84], FRQ (custom antibody ordered from Pel-Freez Biologicals; depleted and used at a dilution of 1:250)[10], and FRH (custom antibody ordered from Pocono Rabbit Farm and Laboratory; used at a dilution of 1:5,000)[5]. V5 antibody (Thermo Pierce), FLAG antibody (Sigma-Aldrich), and HA (Abcam, ab9110) were diluted at 1:5,000 for use as the primary antibody. All uncropped and unprocessed whole blots used for figure preparations were deposited into the Source Data file except for the ones for Supplementary Figure 4a, which were damaged permanently in a lab fire.

Identification of BRD-8 interactors
VHF-tagged BRD-8 were purified with the same method applied for isolation of C-terminal VHF-tagged WC-1[8,62]. 30 g of *Neurospora* tissue (*brd-8*[VHF]) was used for purification of BRD-8. To exclude the possibility that associations with chromatin impacted identification of BRD-8-interactors in purifications, we (1) vortexed lysate at the top speed to mechanically disrupt chromatin: 10 s on/10 s off (put on ice) for a total of 2 min; (2) extensively sonicated protein lysate; (3) included benzonase nuclease in the protein lysis buffer; benzonase is widely used for the removal of nucleic acids (both DNAs and RNAs) from protein samples[85–88]. To recover potential weak interactors, 5 g of tissue from *brd-8*[V5] were purified with V5 antibody (Thermo Pierce)-conjugated Dynabeads (Life Technologies). A single protein band or the whole lane[89] was cut off from the gel as indicated in the figure and used for mass spectrometry analysis.

Mass spectrometry analysis
Affinity purification of BRD-8's interactors using VHF-tagged BRD-8 (the left gel in Fig. 2a) was performed twice (two biological replicates) with similar results, and identification of proteins from excised bands was carried out once with mass spectrometry. Interactor identification from BRD-8[V5] (the middle and right gels in Fig. 2a) was performed three times (three biological replicates), similar band profiles were observed, and specific bands or whole gel lanes were analyzed once by mass spectrometry. Validations for interaction of BRD-8 with its interactors
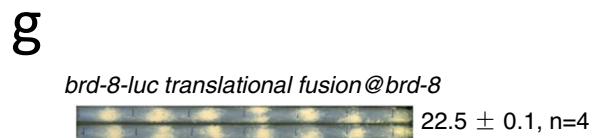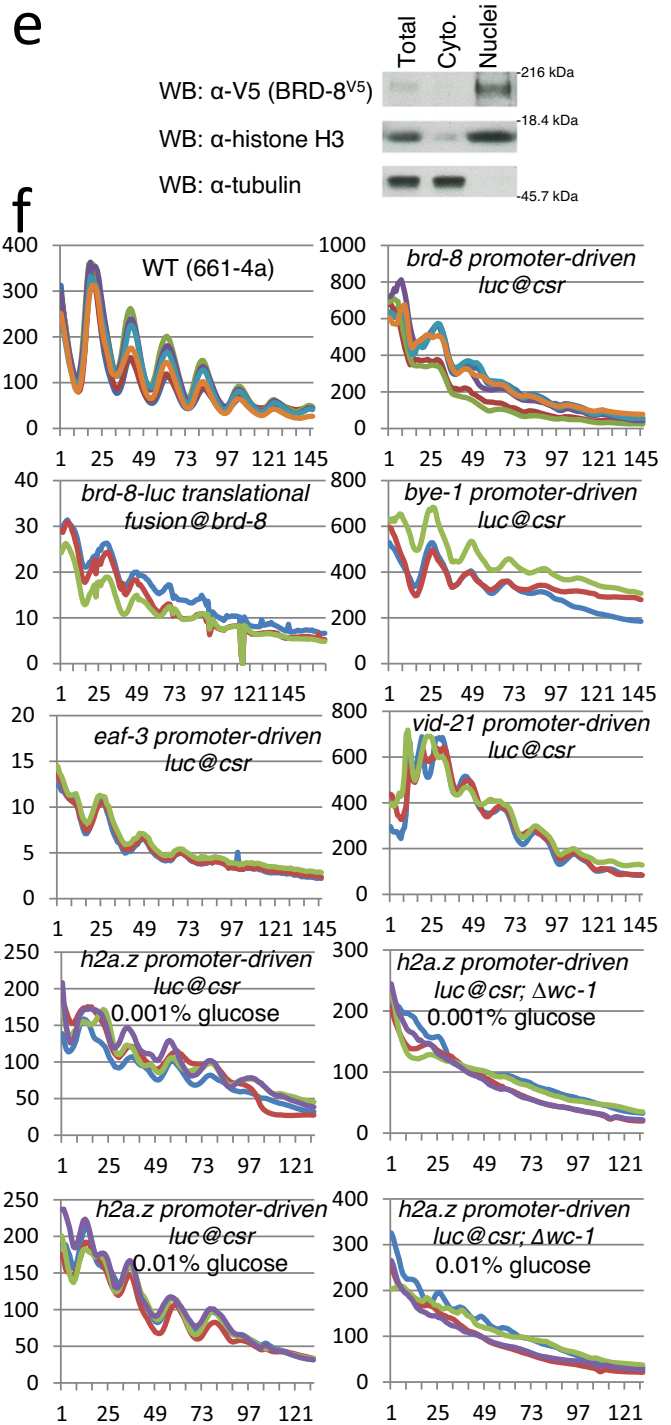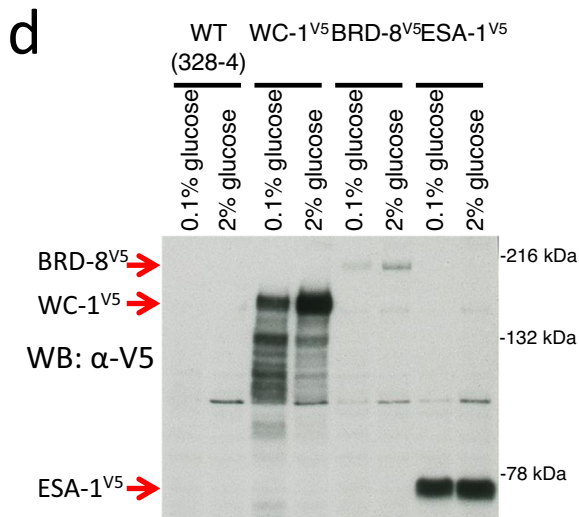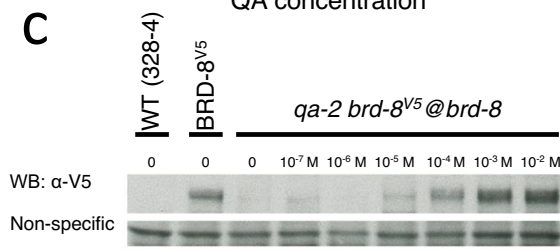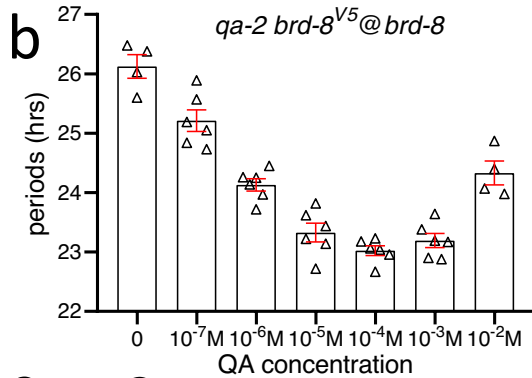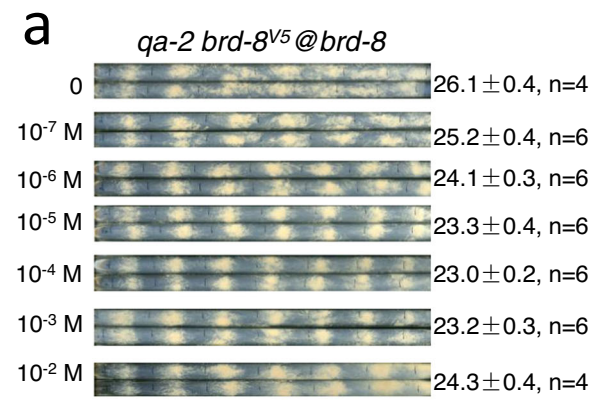
identified from mass spectrometry analyses were performed with strains bearing epitope-tagged target proteins, and results were shown in Fig. 2c. One negative control used in the BRD-8's interactor identification was an untagged *Neurospora* strain (328-4 [*ras-1^bd*, A]). Six samples were analyzed by mass spectrometry.

Samples were separated by SDS-PAGE gel electrophoresis and Coomassie-stained. Gel bands or lanes were excised, destained, and digested with trypsin in 50 mM ammonium bicarbonate overnight at 37 °C. Peptides were extracted using 5% formic acid / 50% acetonitrile (ACN), desalted, and dried. Peptides were analyzed on a Fusion Orbitrap mass spectrometer (Thermo Scientific) equipped with an Easy-nLC 1000 (Thermo Scientific).

Peptides were resuspended in 5% methanol / 1% formic acid and loaded on to an analytical resolving column (35 cm length, 100 µm

Fig. 6 | Characterization of brd-8. a Race tube analysis of *qa-2:brd-8^V5* in the presence of QA at different concentrations as indicated. Strains were cultured on 0.1% glucose race tube medium on race tubes at 25 °C and synchronized by growth in constant light overnight (16-24 hrs) followed by transfer to darkness at the same temperature. **b** Plots of periods of *qa-2:brd-8^V5* in (**a**). Four or six biological replicates of each condition were run and error bars represent standard errors of the means. **c** Western blots showing BRD-8 levels in cultures of *qa-2:brd-8^V5* with different amounts of quinic acid grown in constant light at 25 °C. WT (328-4) and BRD-8^V5 are the negative and positive controls respectively for the Western blots. **d** Western blotting of *brd-8^V5*, *wc-1^V5*, and *esa-1^V5* in cultures grown in different amounts of glucose (0.1 or 2%) in constant light. V5 was inserted to the C-termini of BRD-8, WC-1, and ESA-1 at their native loci respectively, and Western blotting

against the same tag was used to fairly compare their protein levels. Red arrows point to BRD-8^V5, WC-1^V5, and ESA-1^V5 as indicated. **e** Nuclear fractionation of BRD-8^V5 from a culture grown in constant light. The nuclear fractionation was performed as previously described[92]; histone H3 and tubulin were followed as a nuclear and cytoplasm marker respectively. For **c–e**, similar results were observed from three replicates. **f** Bioluminescent analysis of luciferase expression under the control of promoters of *brd-8*, *bye-1*, *eaf-3*, *vid-21*, or *histone h2a.z* at 25 °C; LUC fused to the C terminus of BRD-8 ORF (translational fusion at the locus of *brd-8*) was also measured by the bioluminescent analysis at 25 °C. **g** Race tube analysis of *brd-8*-LUC with 0.1% glucose race tube medium in the dark at 25 °C. Source data were put in the Source Data file.

inner diameter, ReproSil, C18 AQ 3 µm 120 Å pore) pulled in-house (Sutter P-2000, Sutter Instruments, San Francisco, CA) with a 45-min gradient of 5–34% LC-MS buffer B (LC-MS buffer A: 0.0625% formic acid, 3% ACN; LC-MS buffer B: 0.0625% formic acid, 95% ACN). The Fusion Orbitrap was set to perform an Orbitrap MS1 scan (R = 120 K; AGC target = 2.5e5) from 350 to 1,500 m/z, followed by HCD MS2 spectra detected by Orbitrap scanning (R = 15 K; AGC target = 0.5e5; max ion time = 50 ms) for 2 sec before repeating this cycle. Precursor ions were isolated for HCD by quadrupole isolation at width = 0.8 m/z and HCD fragmentation at 29 normalized collision energy (NCE). Charge state 2, 3, and 4 ions were selected for MS2. Precursor ions were added to a dynamic exclusion list ± 10 m ppm for 15 s.

Raw data were searched using COMET[90] in high resolution mode against a target-decoy (reversed)[91] version of the *Neurospora* proteome sequence database (UniProt; downloaded 3/2017) with a precursor mass tolerance of +/− 1 Da and a fragment ion mass tolerance of 0.02 Da, and requiring fully tryptic peptides (K, R; not preceding P) with up to three mis-cleavages. Static modifications included carbamidomethylcysteine and variable modifications included: oxidized methionine. Searches were filtered using orthogonal measures including mass measurement accuracy (+/− 3 ppm), Xcorr for charges from +2 through +4, and dCn targeting a < 1% FDR at the peptide level.

The list of identified interactors (Supplementary Data 1) was searched manually for proteins whose peptides were specifically enriched in the sample of BRD-8^V5 but not in the negative control (328-4, untagged). In the search for BRD-8^V5's interactors, no statistical tests were taken, because we worried that this would rule out certain real targets due to their potential digestion or/and coverage issues in mass spectrometry analysis. Instead, we validated the identified interactors individually by immunoprecipitation assays with epitope-tagged proteins (Fig. 2c).

Immunoprecipitation (IP)

IP was performed as previously described[92,93]. Briefly, 2 mgs of total protein were incubated with 20 µL of V5 agarose (Sigma-Aldrich, Catalog # 7345) or FLAG M2 resin (Sigma-Aldrich, Catalog # A2220) as indicated in the figures, rotating at 4 °C for 2 hrs. The agarose beads were then washed twice with the protein extraction buffer (50 mM HEPES [pH 7.4], 137 mM NaCl, 10% glycerol, 0.4% NP-40) and eluted with 50 µL of 5 × SDS sample buffer at 99 °C for 5 min.

Chromatin immunoprecipitation (ChIP)

ChIP experiments were done as previously described using fresh tissues[62]. Primer sets against *C-box* and *pLRE* were the same as in a previous publication[8]. Primer sets against the *frq* locus used in Fig. 4a were derived from a previous publication[94]. "A" in the first "ATG" of the full-length *frq* coding region is designated as "+1" and the upstream nucleotides are labeled "-" accordingly (without "0"). *frq C-box* is from −2,878 to −2,624 nt, the amplicon with the *frq1* primer set is from −2,754 to −2,644 nt, while that by the *C-box* primer set is from −2,790 to −2,678 nt. ChIP using *Neurospora* tissue: *Neurospora* tissue was cross-

linked with 3% formaldehyde for 15 min and quenched with 0.25 M glycine for 5 min. Tissue was then washed with PBS three times and vacuum-dried; 0.4 g was weighed, cut into 9 pieces, and each piece soaked in 0.5 ml SDS lysis buffer (50 mM Tris/HCL [pH 8.0], 1% SDS, 5 mM EDTA) containing Roche protease inhibitors (Sigma-Aldrich, Catalog # 11836170001). The soaked tissue was first sonicated for 8 sec for three times at 30% amplitude with a Bronson sonicator equipped with a microtip, and then further sonicated in a water-bath sonicator 5 times for 5 min each with an interval of 30 sec on and 30 sec off. The sonicated cell lysate was cleared of cellular debris by an 8,000 rpm centrifugation twice for 5 min each. 200 µl supernatant was saved and added to 1.8 ml RIPA buffer; 15 µL protein A magnetic beads and 2 µL V5 antibody (Abcam, Catalog # ab9116) were added to the mixture followed by rotation at 4 °C overnight. The following morning, immunoprecipitated DNA was washed with buffers A-D (buffer A: 20 mM Tris/HCL [pH 8.0], 0.1% SDS, 2 mM EDTA, 1% TritonX-100; buffer B: 20 mM Tris/HCL [pH 8.0], 0.1% SDS, 2 mM EDTA, 1% TritonX-100, 500 mM NaCl; buffer C: 10 mM Tris/HCL [pH 8.0], 0.25 M LiCl, 1 mM EDTA, 1% TritonX-100, 1% sodium deoxycholate; buffer D: 10 mM Tris/HCL [pH 8.0], 1 mM EDTA) once each, eluted with Elution buffer (0.1 M NaHCO₃, 1% SDS), reverse crosslinked with NaCl at the final concentration of 0.2 M, and purified with Qiagen PCR purification kit.

Ion ChIP-Seq Library Preparation

The purified ChIP DNA was end-repaired and ligated to Ion-compatible barcode adapters using Ion XpressTM Plus Fragment Kit (Catalog # 4471269) and Ion XpressTM Barcode Adapters (Catalog # 4471250). The final libraries were purified with two rounds of AMPure XP Bead capture to size select fragments between 160 to 340 bps in length. The emulsion clonal bead amplification to generate bead templates for the Ion Torrent platform was performed on the Ion Chef System (Thermo Fisher Scientific) with the Ion PI™ Hi-Q™ Chef Kit (Thermo Fisher Scientific, Catalog # A27198) and Ion PI™ Chip Kit v3 (Thermo Fisher Scientific, Catalog # A26771). Sequencing was done using the Ion PI™ Hi-Q™ Sequencing 200 Kit (Thermo Fisher Scientific, Catalog # A26772) on Ion Proton sequencer with sequencing data processing using the Torrent Suite TM Software (Ver. 4.0.2) on the Torrent server.

Samples were mapped to the *Neurospora crassa* genome (from GenBank) using TMAP (Ion Software, https://github.com/iontorrent/TMAP). Mapping efficiency and read quality were visualized using htseq-qa (http://htseq.readthedocs.io/en/release_0.9.1/). Peaks were called using MACS2 (https://github.com/taoliu/MACS), and peaks were annotated with ChIPseeker (Bioconductor, https://bioconductor.org/packages/release/bioc/html/ChIPseeker.html). In addition to MACS2, the SICER software (https://home.gwu.edu/~wpeng/Software.htm) was used to identify peaks and identify differentially abundant peaks between WT and mutant strains. For comparison of WT vs. control in histone and acetylated histone, three runs apiece were performed with window sizes of 200, 400 and 600, and gap sizes of 600, 1,200 and 1,800, respectively. Redundant peaks between the three runs (within 2,500 bp) were eliminated with a simple R script.
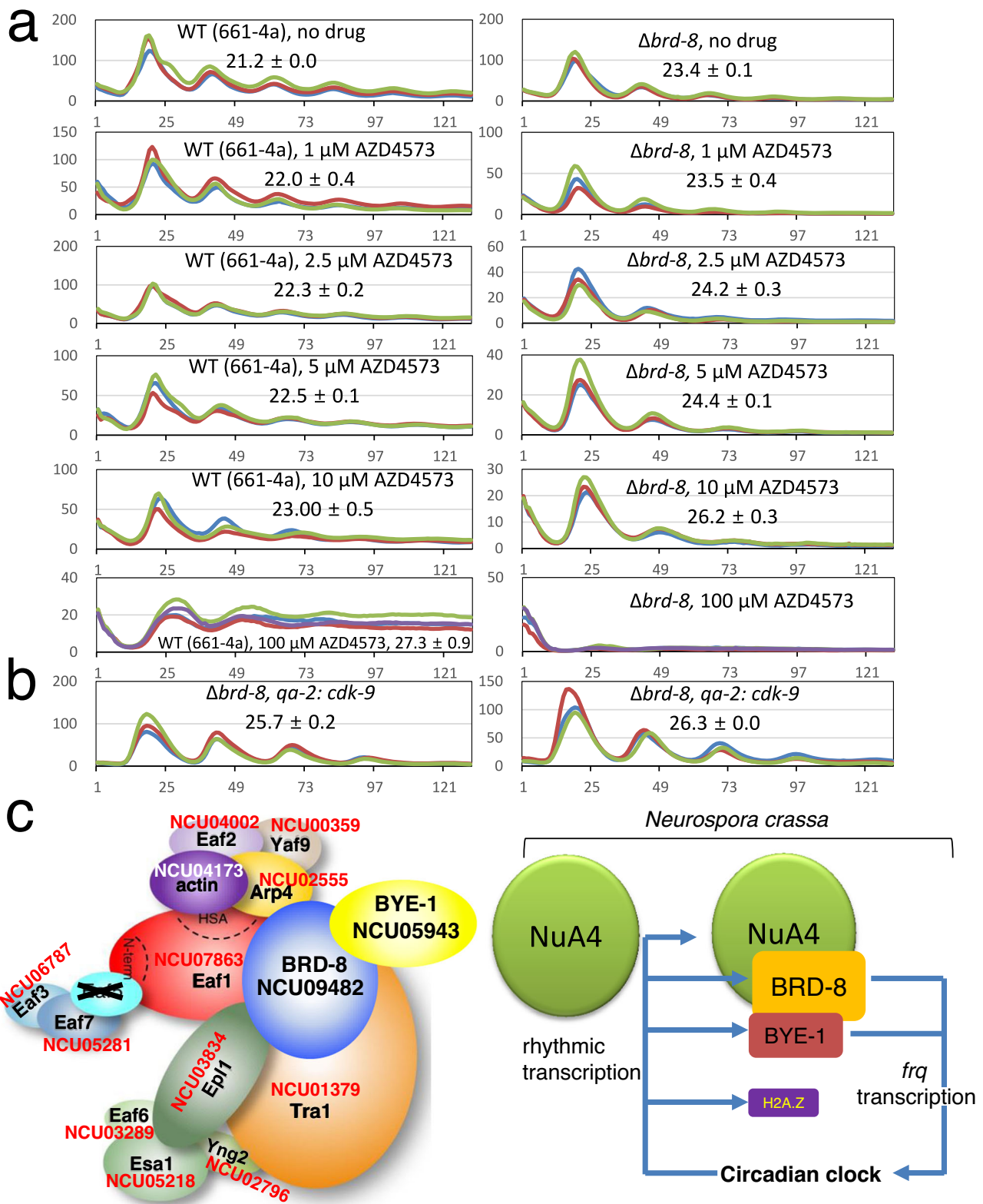
Another script was used to identify genes within 1,000 bp from either border of the peaks.

Histone acetylation assay in vitro

The histone acetylation assay was performed as previously described with modifications[95]. Briefly, ESA-1 was immunoprecipitated from the *esa-1*^{V5} strain as described in the section of "IP" with V5 antibody-conjugated resins. Immunoprecipitated- ESA-1^{V5}-bound resins were washed twice with phosphate buffered saline containing 0.1% Tween 20 and once with the acetyl-transferase assay buffer (50 mM Tris-Cl [pH 8.0], 10% glycerol, 10 mM butyric acid, 0.1 mM EDTA, 1 mM DTT, 1 mM PMSF). 50 µL of the acetyl-transferase assay buffer containing 10 µM acetyl CoA (Sigma-Aldrich) was added to the washed resins. Recombinant human histone H2A (New England BioLabs, Catalog #

Fig. 7 | Impairment of transcription elongation lengthens circadian period, leading to a model in which BRD-8 and BYE-1, in complex with NuA4 subunits, maintain circadian period length. a Pharmacological inhibition of CDK-9 results in period lengthening and further lengthens the circadian period of Δ*brd-8*. Bioluminescent analysis of WT and Δ*brd-8* in the presence or absence of AZD4573, an inhibitor of CDK-9, at concentrations of 0, 1, 2.5, 5, 10, and 100 μM as indicated in the figure. AZD4573 was added to 0.1% glucose race-tube medium in a 96-well plate to the final concentrations indicated, and strains inoculated and grown in the light at 25 °C overnight were transferred to the dark at the same temperature to record bioluminescent signals. **b** Genetic downregulation of CDK-9 results in period lengthening. Bioluminescent analysis of two independent Δ*brd-8* strains in which the promoter of *cdk-9* was replaced by the *qa-2* promoter to down-regulate

expression of *cdk-9* when QA was absent in the medium. **c** Working model. On the left is the conceptual model of the NuA4 complex described here, modified from previous work (Wang, X., Ahmad, S., Zhang, Z. et al. Architecture of the *Saccharomyces cerevisiae* NuA4/TIP60 complex. *Nat Commun* **9**, 1147 [2018]. https://doi.org/10.1038/s41467-018-03504-5)[97] to add auxiliary subunits BRD-8 and BYE-1 and to show interactions established here along with the corresponding *Neurospora* gene numbers; Eaf5 is crossed out to reflect its absence (Supplementary Fig. 5). Right: there are at least two types of NuA4 complexes in *Neurospora* with or without BRD-8 and BYE-1. BRD-8 and BYE-1 are required for normal *frq* transcription and circadian period determination; transcription of *brd-8*, *bye-1*, *eaf-3*, *vid-21*, and *histone h2a.z* are under circadian control.

M2502S) or H4 (New England BioLabs, Catalog # M2504S) respectively was added to the mixture at a final concentration of 0.1 mg/mL. Acetylation reactions were incubated at 30 °C for 1 hr, followed by adding 50 μL of 5 x SDS-PAGE sample buffer, heated at 99 °C for 5 min, electrophoresed in a 4-12% bis-tris SDS-PAGE gel, and transferred to a PVDF membrane. Acetylated histones H4 and H2A were detected by immunoblotting with rabbit anti-acH4 (UBI, Catalog # 06–866, 1:1000 dilution) and anti-acH2A K9 (Millipore Sigma, Catalog # 07-289), respectively.

RT-quantitative PCR

Neurospora mRNA was isolated with TRIzol reagent (Life Technologies) and cDNA synthesis was done using SuperScript III first strand synthesis kit (Life Technologies) with 3 μg of purified RNA[47]. Real-time PCR was performed with QuantiTect SYBR green RT-PCR kit (Qiagen) in an ABI 7500 Fast system. Primers against *frq* and *wc-1* genes were from previous publications[47,96]. Normalization for RT-qPCR was to NCU08964, a gene identified previously as among the most constantly expressed under different conditions and times or day, and least responsive to changes in media[40].

Other techniques

Mass spectrometry was performed as previously described[62]. Luciferase assays were performed as previously described[8,81]. If QA was used in the luciferase assay, it was indicated in the figures. Nuclear preparation was performed as reported[92].

Reporting summary

Further information on research design is available in the Nature Portfolio Reporting Summary linked to this article.

Data availability

The data that support this study are available from the corresponding authors upon reasonable request. The mass spectrometry and ChIP-sequencing data generated in this study have been deposited in the MassIVE database under accession: MSV000089415 (ProteomeXchange PXD033576) and NCBI SRA under accession: PRJNA834768, respectively. Source data are provided with this paper.

References

1. He, Q. et al. White collar-1, a DNA binding transcription factor and a light sensor. *Science* **297**, 840–843 (2002).
2. Froehlich, A. C., Loros, J. J. & Dunlap, J. C. Rhythmic binding of a WHITE COLLAR-containing complex to the frequency promoter is inhibited by FREQUENCY. *Proc. Natl Acad. Sci.* **100**, 5914–5919 (2003).
3. Froehlich, A. C., Liu, Y., Loros, J. J. & Dunlap, J. C. White Collar-1, a Circadian blue light photoreceptor, binding to the frequency promoter. *Science* **297**, 815–819 (2002).
4. Cheng, P., He, Q., He, Q., Wang, L. & Liu, Y. Regulation of the Neurospora circadian clock by an RNA helicase. *Genes Dev.* **19**, 234–241 (2005).
5. Shi, M., Collett, M., Loros, J. J. & Dunlap, J. C. FRQ-Interacting RNA helicase mediates negative and positive feedback in the neurospora circadian clock. *Genetics* **184**, 351–361 (2010).
6. He, Q. et al. CKI and CKII mediate the FREQUENCY-dependent phosphorylation of the WHITE COLLAR complex to close the Neurospora circadian negative feedback loop. *Genes Dev.* **20**, 2552–2565 (2006).
7. Baker, C. L., Kettenbach, A. N., Loros, J. J., Gerber, S. A. & Dunlap, J. C. Quantitative proteomics reveals a dynamic interactome and phase-specific phosphorylation in the Neurospora circadian clock. *Mol. Cell* **34**, 354–363 (2009).
8. Wang, B., Kettenbach, A. N., Zhou, X., Loros, J. J. & Dunlap, J. C. The phospho-code determining circadian feedback loop closure and output in Neurospora. *Mol. Cell* **74**, 771–784 (2019).
9. Schafmeier, T. et al. Transcriptional feedback of neurospora circadian clock gene by phosphorylation-dependent inactivation of its transcription factor. *Cell* **122**, 235–246 (2005).
10. Garceau, N. Y., Liu, Y., Loros, J. J. & Dunlap, J. C. Alternative initiation of translation and time-specific phosphorylation yield multiple forms of the essential clock protein FREQUENCY. *Cell* **89**, 469–476 (1997).
11. Ferraro, A. R. et al. Chromatin accessibility profiling in Neurospora crassa reveals molecular features associated with accessible and inaccessible chromatin. *BMC Genomics* **22**, 459 (2021).
12. Jiang, C. & Pugh, B. F. Nucleosome positioning and gene regulation: advances through genomics. *Nat. Rev. Genet* **10**, 161–172 (2009).
13. Sterner, D. E. & Berger, S. L. Acetylation of histones and transcription-related factors. *Microbiol Mol. Biol. Rev.* **64**, 435–459 (2000).
14. Becker, P. B. & Workman, J. L. Nucleosome remodeling and epigenetics. *Cold Spring Harb Perspect Biol* **5**, a017905 (2013).
15. Jonkers, I. & Lis, J. T. Getting up to speed with transcription elongation by RNA polymerase II. *Nat. Rev. Mol. Cell Biol.* **16**, 167–177 (2015).
16. Allard, S. et al. NuA4, an essential transcription adaptor/histone H4 acetyltransferase complex containing Esa1p and the ATM-related cofactor Tra1p. *EMBO J.* **18**, 5108–5119 (1999).
17. Chittuluru, J. R. et al. Structure and nucleosome interaction of the yeast NuA4 and Piccolo-NuA4 histone acetyltransferase complexes. *Nat. Struct. Mol. Biol.* **18**, 1196–1203 (2011).
18. Xu, P. et al. The NuA4 core complex acetylates nucleosomal histone H4 through a double recognition mechanism. *Mol. Cell* **63**, 965–975 (2016).
19. Altaf, M. et al. NuA4-dependent acetylation of nucleosomal histones H4 and H2A directly stimulates incorporation of H2A.Z by the SWR1 cComplex. *J. Biol. Chem.* **285**, 15966–15977 (2010).
20. Ginsburg, D. S., Govind, C. K. & Hinnebusch, A. G. NuA4 lysine acetyltransferase Esa1 is targeted to coding regions and stimulates transcription elongation with Gcn5. *Mol. Cell Biol.* **29**, 6473–6487 (2009).
21. Doyon, Y., Selleck, W., Lane, W. S., Tan, S. & Côté, J. Structural and functional conservation of the NuA4 histone acetyltransferase

complex from yeast to humans. *Mol. Cell Biol.* **24**, 1884–1896 (2004).

22. Cai, Y. et al. Identification of new subunits of the multiprotein mammalian TRRAP/TIP60-containing histone acetyltransferase complex. *J. Biol. Chem.* **278**, 42733–42736 (2003).

23. Petkau, N., Budak, H., Zhou, X., Oster, H. & Eichele, G. Acetylation of BMAL1 by TIP60 controls BRD4-P-TEFb recruitment to circadian promoters. *eLife* **8**, e43235 (2019).

24. Wu, X., Rossettini, A. & Hanes, S. D. The ESS1 prolyl isomerase and its suppressor BYE1 interact with RNA pol II to inhibit transcription elongation in Saccharomyces cerevisiae. *Genetics* **165**, 1687–1702 (2003).

25. Pinskaya, M. et al. PHD and TFIIS-Like domains of the Bye1 transcription factor determine its multivalent genomic distribution. *PLoS One* **9**, e102464 (2014).

26. Kinkelin, K. et al. Structures of RNA polymerase II complexes with Bye1, a chromatin-binding PHF3/DIDO homologue. *Proc. Natl Acad. Sci. USA* **110**, 15277–15282 (2013).

27. Shogren-Knaak, M. et al. Histone H4-K16 acetylation controls chromatin structure and protein interactions. *Science* **311**, 844–847 (2006).

28. Fraga, M. F. et al. Loss of acetylation at Lys16 and trimethylation at Lys20 of histone H4 is a common hallmark of human cancer. *Nat. Genet.* **37**, 391–400 (2005).

29. Peleg, S. et al. Altered histone acetylation is associated with age-dependent memory impairment in mice. *Science* **328**, 753–756 (2010).

30. Bahari-Javan, S., Sananbenesi, F. & Fischer, A. Histone-acetylation: a link between Alzheimer's disease and post-traumatic stress disorder? *Front. Neurosci.* **8**, 160 (2014).

31. Bird, A. W. et al. Acetylation of histone H4 by Esa1 is required for DNA double-strand break repair. *Nature* **419**, 411–415 (2002).

32. Squatrito, M., Gorrini, C. & Amati, B. Tip60 in DNA damage response and growth control: many tricks in one HAT. *Trends Cell Biol.* **16**, 433–442 (2006).

33. Sun, Y., Jiang, X., Chen, S., Fernandes, N. & Price, B. D. A role for the Tip60 histone acetyltransferase in the acetylation and activation of ATM. *Proc. Natl Acad. Sci.* **102**, 13182–13187 (2005).

34. Espinosa-Cores, L. et al. Insights into the function of the NuA4 Complex in Plants. *Front. Plant Sci.* **11**, 125 (2020).

35. Murr, R. et al. Histone acetylation by Trrap–Tip60 modulates loading of repair proteins and repair of DNA double-strand breaks. *Nat. Cell Biol.* **8**, 91–99 (2006).

36. Valdés-Mora, F. et al. Acetylated histone variant H2A.Z is involved in the activation of neo-enhancers in prostate cancer. *Nat. Commun.* **8**, 1346 (2017).

37. Valdés-Mora, F. et al. Acetylation of H2A.Z is a key epigenetic modification associated with gene deregulation and epigenetic remodeling in cancer. *Genome Res.* **22**, 307–321 (2012).

38. Mandemaker, I. K. et al. DNA damage-induced replication stress results in PA200-proteasome-mediated degradation of acetylated histones. *EMBO Rep.* **19**, e45566 (2018).

39. Vettese-Dadey, M. et al. Acetylation of histone H4 plays a primary role in enhancing transcription factor binding to nucleosomal DNA in vitro. *EMBO J.* **15**, 2508–2518 (1996).

40. Seligson, D. B. et al. Global histone modification patterns predict risk of prostate cancer recurrence. *Nature* **435**, 1262–1266 (2005).

41. Gonzales-Cope, M., Sidoli, S., Bhanu, N. V., Won, K.-J. & Garcia, B. A. Histone H4 acetylation and the epigenetic reader Brd4 are critical regulators of pluripotency in embryonic stem cells. *BMC Genomics* **17**, 95 (2016).

42. Megee, P. C., Morgan, B. A. & Smith, M. M. Histone H4 and the maintenance of genome integrity. *Genes Dev.* **9**, 1716–1727 (1995).

43. Román, A.-C. et al. Histone H4 acetylation regulates behavioral inter-individual variability in zebrafish. *Genome Biol.* **19**, 55 (2018).

44. Molina-Serrano, D. et al. Loss of Nat4 and its associated histone H4 N-terminal acetylation mediates calorie restriction-induced longevity. *EMBO Rep.* **17**, 1829–1843 (2016).

45. Dunlap, J. C. et al. Enabling a community to dissect an organism: Overview of the neurospora functional genomics project. *Adv. Genetics*. **57**, 49–96 (Elsevier, 2007).

46. Belden, W. J. et al. The band mutation in Neurospora crassa is a dominant allele of ras-1 implicating RAS signaling in circadian output. *Genes Dev.* **21**, 1494–1505 (2007).

47. Chen, C.-H., Ringelberg, C. S., Gross, R. H., Dunlap, J. C. & Loros, J. J. Genome-wide analysis of light-inducible responses reveals hierarchical light signalling in Neurospora. *EMBO J.* **28**, 1029–1042 (2009).

48. Cheng, P., Yang, Y. & Liu, Y. Interlocked feedback loops contribute to the robustness of the Neurospora circadian clock. *Proc. Natl Acad. Sci. USA* **98**, 7408–7413 (2001).

49. Doyon, Y. & Côté, J. The highly conserved and multifunctional NuA4 HAT complex. *Curr. Opin. Genet. Dev.* **14**, 147–154 (2004).

50. Eisen, A. et al. The yeast NuA4 and drosophila MSL complexes contain homologous subunits important for transcription regulation. *J. Biol. Chem.* **276**, 3484–3491 (2001).

51. Liu, H. et al. A-to-I RNA editing is developmentally regulated and generally adaptive for sexual reproduction in Neurospora crassa. *Proc. Natl Acad. Sci. USA* **114**, E7756–E7765 (2017).

52. Bian, Z., Ni, Y., Xu, J.-R. & Liu, H. A-to-I mRNA editing in fungi: occurrence, function, and evolution. *Cell. Mol. Life Sci.* **76**, 329–340 (2019).

53. Yan, Y., Barlev, N. A., Haley, R. H., Berger, S. L. & Marmorstein, R. Crystal structure of yeast Esa1 suggests a unified mechanism for catalysis and substrate binding by histone acetyltransferases. *Mol. Cell* **6**, 1195–1205 (2000).

54. Devoucoux, M. et al. MRG proteins are shared by multiple protein complexes with distinct functions. *Mol. Cell. Proteom.* **21**, 100253 (2022).

55. Hurley, J. M. et al. Circadian proteomic analysis uncovers mechanisms of post-transcriptional regulation in metabolic pathways. *Cell Syst.* **7**, 613–626.e5 (2018).

56. Cidado, J. et al. AZD4573 is a highly selective CDK9 inhibitor that suppresses MCL-1 and induces apoptosis in hematologic cancer cells. *Clin. Cancer Res.* **26**, 922–934 (2020).

57. Bhatt, S. et al. Reduced mitochondrial apoptotic priming drives resistance to BH3 mimetics in acute myeloid leukemia. *Cancer Cell* **38**, 872–890.e6 (2020).

58. Barlaam, B. et al. Discovery of AZD4573, a potent and selective inhibitor of CDK9 that enables short duration of target engagement for the treatment of hematological malignancies. *J. Med. Chem.* **63**, 15564–15590 (2020).

59. Pike, K. G. et al. Polycyclic amide derivatives as CDK9 inhibitors, Patent WO2017001354; 2017.

60. Belden, W. J., Loros, J. J. & Dunlap, J. C. Execution of the circadian negative feedback loop in Neurospora requires the ATP-dependent chromatin-remodeling enzyme CLOCKSWITCH. *Mol. Cell* **25**, 587–600 (2007).

61. Belden, W. J., Lewis, Z. A., Selker, E. U., Loros, J. J. & Dunlap, J. C. CHD1 remodels chromatin and influences transient DNA methylation at the clock gene frequency. *PLoS Genet* **7**, e1002166 (2011).

62. Wang, B., Kettenbach, A. N., Gerber, S. A., Loros, J. J. & Dunlap, J. C. Neurospora WC-1 recruits SWI/SNF to remodel frequency and initiate a circadian Cycle. *PLOS Genet.* **10**, e1004599 (2014).

63. Cha, J., Zhou, M. & Liu, Y. CATP is a critical component of the Neurospora circadian clock by regulating the nucleosome occupancy rhythm at the frequency locus. *EMBO Rep.* **14**, 923–930 (2013).

64. Cao, X. et al. Transcription factor CBF-1 is critical for circadian gene expression by modulating WHITE COLLAR complex recruitment to the frq locus. *PLoS Genet* **14**, e1007570 (2018).

65. Gai, K. et al. Transcriptional repression of frequency by the IEC-1-INO80 complex is required for normal Neurospora circadian clock function. *PLoS Genet* **13**, e1006732 (2017).

66. Lee, K. K. & Workman, J. L. Histone acetyltransferase complexes: one size doesn't fit all. *Nat. Rev. Mol. Cell Biol.* **8**, 284–295 (2007).

67. Kamei, M. et al. IMITATION SWITCH is required for normal chromatin structure and gene repression in PRC2 target domains. *Proc. Natl Acad. Sci. USA* **118**, e2010003118 (2021).

68. Courtney, A. J. et al. Normal patterns of histone H3K27 methylation require the histone variant H2A.Z in *Neurospora crassa*. *Genetics* **216**, 51–66 (2020).

69. Ferraro, A. R. & Lewis, Z. A. ChIP-Seq Analysis in Neurospora crassa. in *Fungal* Genomics (eds. de Vries, R. P., Tsang, A. & Grigoriev, I. V.). 1775 241–250 (Springer New York, 2018).

70. Raduwan, H., Isola, A. L. & Belden, W. J. Methylation of histone H3 on lysine 4 by the lysine methyltransferase SET1 protein is needed for normal clock gene expression. *J. Biol. Chem.* **288**, 8380–8390 (2013).

71. Shevchenko, A. et al. Chromatin Central: towards the comparative proteome by accurate mapping of the yeast proteomic environment. *Genome Biol.* **9**, R167 (2008).

72. Brenna, A., Grimaldi, B., Filetici, P. & Ballario, P. Physical association of the WC-1 photoreceptor and the histone acetyltransferase NGF-1 is required for blue light signal transduction in *Neurospora crassa*. *MBoC* **23**, 3863–3872 (2012).

73. Shu, S. et al. Synthetic lethal and resistance interactions with BET bromodomain inhibitors in triple-negative breast cancer. *Mol. Cell* **78**, 1096–1113.e8 (2020).

74. Takahashi, J. S. Transcriptional architecture of the mammalian circadian clock. *Nat. Rev. Genet* **18**, 164–179 (2017).

75. Koike, N. et al. Transcriptional architecture and chromatin landscape of the core circadian clock in mammals. *Science* **338**, 349–354 (2012).

76. Brunner, M. & Schafmeier, T. Transcriptional and post-transcriptional regulation of the circadian clock of cyanobacteria and *Neurospora*. *Genes Dev.* **20**, 1061–1074 (2006).

77. Kim, Y. H. et al. Rev-erbα dynamically modulates chromatin looping to control circadian gene transcription. *Science* **359**, 1274–1277 (2018).

78. Papazyan, R., Zhang, Y. & Lazar, M. A. Genetic and epigenomic mechanisms of mammalian circadian transcription. *Nat. Struct. Mol. Biol.* **23**, 1045–1052 (2016).

79. Koronowski, K. B. & Sassone-Corsi, P. Communicating clocks shape circadian homeostasis. *Science* **371**, eabd0951 (2021).

80. Wang, B. & Dunlap, J. C. Domains Required for the Interaction of the Central Negative Element FRQ with its Transcriptional Activator WCC within the Core Circadian Clock of Neurospora. *J. Biol. Chem.* https://doi.org/10.1016/j.jbc.2023.104850 (2023).

81. Wang, B., Zhou, X., Gerber, S. A., Loros, J. J. & Dunlap, J. C. Cellular Calcium Levels Influenced by NCA-2 Impact Circadian Period Determination in *Neurospora*. *mBio* **12**, e0149321 (2021).

82. Zhou, X. et al. A HAD family phosphatase CSP-6 regulates the circadian output pathway in Neurospora crassa. *PLoS Genet* **14**, e1007192 (2018).

83. Lee, K., Dunlap, J. C. & Loros, J. J. Roles for WHITE COLLAR-1 in circadian and general photoperception in *Neurospora crassa*. *Genetics* **163**, 103–114 (2003).

84. Denault, D. L. WC-2 mediates WC-1-FRQ interaction within the PAS protein-linked circadian feedback loop of Neurospora. *EMBO J.* **20**, 109–117 (2001).

85. Liu, Z. & Myers, L. C. Fungal mediator tail subunits contain classical transcriptional activation domains. *Mol. Cell Biol.* **35**, 1363–1375 (2015).

86. Mundle, S. T. et al. High-purity preparation of HSV-2 vaccine candidate ACAM529 is immunogenic and efficacious in vivo. *PLoS ONE* **8**, e57224 (2013).

87. Rizzo, M. A., Springer, G. H., Granada, B. & Piston, D. W. An improved cyan fluorescent protein variant useful for FRET. *Nat. Biotechnol.* **22**, 445–449 (2004).

88. MacAlpine, J. et al. A small molecule produced by Lactobacillus species blocks Candida albicans filamentation by inhibiting a DYRK1-family kinase. *Nat. Commun.* **12**, 6151 (2021).

89. Liu, H.-L. et al. Single-step affinity purification for fungal proteomics. *Eukaryot. Cell* **9**, 831–833 (2010).

90. Eng, J. K., Jahan, T. A. & Hoopmann, M. R. Comet: An open-source MS/MS sequence database search tool. *Proteomics* **13**, 22–24 (2013).

91. Elias, J. E. & Gygi, S. P. Target-decoy search strategy for increased confidence in large-scale protein identifications by mass spectrometry. *Nat. Methods* **4**, 207–214 (2007).

92. Wang, B., Zhou, X., Loros, J. J. & Dunlap, J. C. Alternative use of DNA binding domains by the neurospora white collar complex dictates circadian regulation and light responses. *Mol. Cell. Biol.* **36**, 781–793 (2016).

93. Wang, B., Stevenson, E.-L. & Dunlap, J. C. Functional analysis of 110 phosphorylation sites on the circadian clock protein FRQ identifies clusters determining period length and temperature compensation. *G3 Genes|Genomes|Genet.* **13**, jkac334 (2023).

94. Xue, Z. et al. Transcriptional interference by antisense RNA is required for circadian clock function. *Nature* **514**, 650–653 (2014).

95. Kuninger, D., Lundblad, J., Semirale, A. & Rotwein, P. A non-isotopic in vitro assay for histone acetylation. *J. Biotechnol.* **131**, 253–260 (2007).

96. Chen, C.-H., DeMay, B. S., Gladfelter, A. S., Dunlap, J. C. & Loros, J. J. Physical interaction between VIVID and white collar complex regulates photoadaptation in Neurospora. *Proc. Natl Acad. Sci. USA* **107**, 16715–16720 (2010).

97. Wang, X., Ahmad, S., Zhang, Z., Côté, J. & Cai, G. Architecture of the Saccharomyces cerevisiae NuA4/TIP60 complex. *Nat. Commun.* **9**, 1147 (2018).

Acknowledgements

Author contributions

Conceived and designed the experiments: BW, JJL, JCD. Performed the experiments: BW, XYZ, ANK, HDM, LMM. Analyzed the data: BW, XYZ, ANK, HDM, LMM, JJL, and JCD. Contributed reagents/materials/analysis tools: BW, XYZ, ANK, HDM, and LMM. Wrote the paper: BW and JCD.

Competing interests

The authors declare no competing interests.

Additional information

Supplementary information The online version contains supplementary material available at https://doi.org/10.1038/s41467-023-38817-7.

Correspondence and requests for materials should be addressed to Bin Wang or Jay C. Dunlap.

Peer review information *Nature Communications* thanks the anonymous reviewers for their contribution to the peer review of this work. A peer review file is available.

Reprints and permissions information is available at http://www.nature.com/reprints

Publisher's note Springer Nature remains neutral with regard to jurisdictional claims in published maps and institutional affiliations.